Mechanical and Electrical Stimulation for Tissue Engineered Skeletal Muscle

---

Major Qualifying Project Submitted to the Faculty of WPI in partial fulfillment of the requirements for the Degree of Bachelor of Science

Authored by:

Michael Antonelli

Lyra Huynh

Deborah Kalambayi

Nicholas Seagrave

Lara Schmoyer

Advisors: Professor Raymond Page, Ph.D. & Professor Marko Popovic, Ph.D.

April 28, 2019

Abstract

The human skeletal system is composed of over 640 muscles and is responsible for producing movement, maintaining posture, stabilizing joints, maintaining homeostasis and protecting internal organs. Any chronic or major damage to this system can hinder these functions and impair basic daily activities. Currently, 1.7 billion people worldwide are affected by musculoskeletal conditions. In addition, 90% of investigational drugs fail phase 2 clinical trials due to lack of efficacy on muscular effects. Animal models and present 2D and 3D in vitro models are not accurate representations of *in vivo* human muscles. This project aims to design and construct a multi-well construct to grow and fully mature 3D human skeletal muscle tissues for drug testing by mechanically and electrically stimulating the tissues to mimic natural environmental conditions. This design adapted Vandenburg's microposts and incorporated air chambers with electrical air pumps to deflect the microposts. The apparatus was tested for proof of concept, a correlation profile was drawn for pressure and deflection, and force generated was calculated. Electrical voltages were recorded from the electrodes for a stimulation regimen.

Acknowledgements

The team would like to give thanks to our MQP advisor Raymond Page, PhD for his guidance throughout the project. In addition, we would like to acknowledge Lisa Wall (Lab Manager) for her support and reliability, Ying Lei (WPI PhD Candidate) for her assistance in the fabrication of PDMS microposts, and Marko Popovic, PhD for his advice in the design process.

Executive Summary

I. Introduction

1.7 billion people worldwide suffer from various muscle diseases, such as Type 1 Myotonic Dystrophy, Duchenne muscle dystrophy, sarcopenia and Polymyositis, some of which can prove fatal [1,2,3,4,5,6]. There is a need for new and improved medicines to treat these diseases. However, 90% of new investigational drugs fail phase 2 clinical trials due to lack of efficacy [7]. To avoid wasting time and resources, scientists have developed some methods to test drugs prior to releasing them for clinical trials. Some existing methods include using animal tissue and human donor tissues. However, the usage of animal tissues is flawed because animals are physiologically different from humans and donor tissue is difficult to acquire in reasonably large amounts and involve many complications based on the different tissue sources.

Therefore, the best candidate for mass-production of experimental tissue would be lab-grown tissue, or tissue engineered skeletal muscle (TESM). However, this method also has limitations because of the complications of growing TESMs in a way that would replicate the characteristics of native human skeletal muscle. Some complications include low thickness, small diameter, low fiber strength and lack of migration of nuclei [8].

The goal of this project is to properly mature 3D TESM and achieve the physiological and morphological characteristics of *in vivo* skeletal muscle tissue. To achieve this, the team will use mechanical and electrical stimulation at different frequencies and evaluate the contractile force generated.

II. Device Design

Based on the client's statement, the team was able to map the objectives shown in Figure ES1 below.

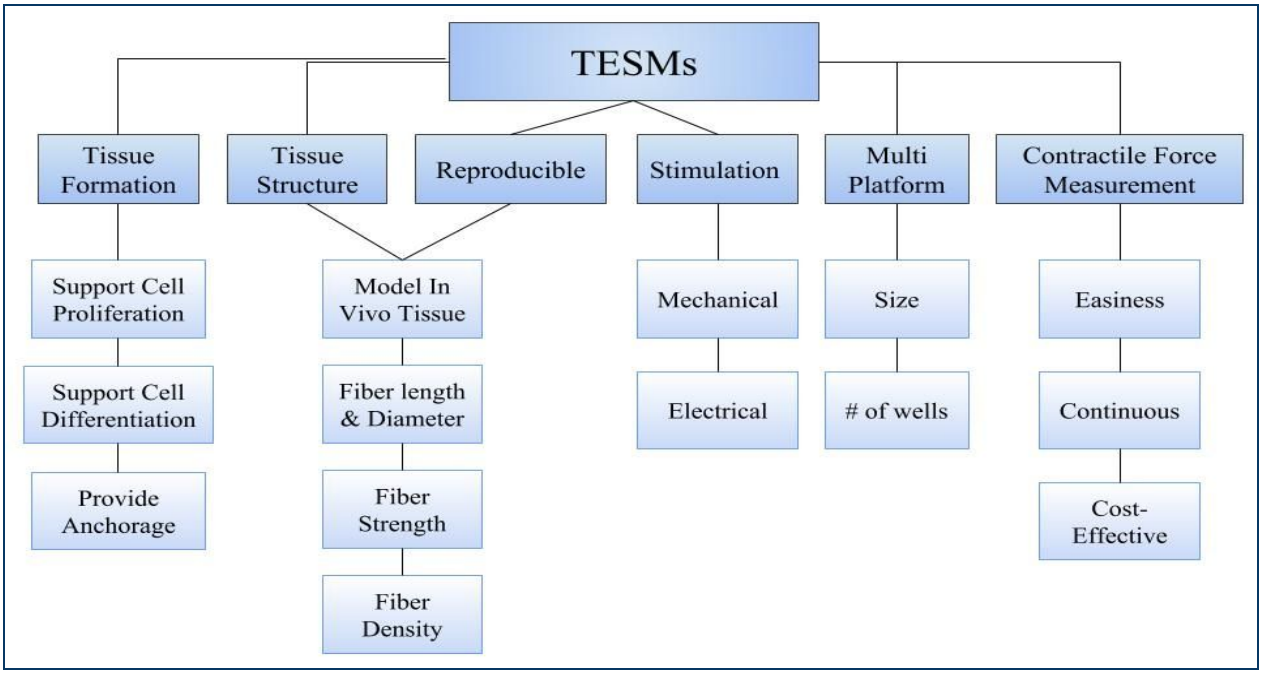

Figure ES1. Concept map.

Alternative Designs

The team came up with three alternative designs that could accomplish the objectives, which are described below.

Wells and pegged/bumped base

The design consists of a bottomless 96 well plate and a 3D-printed base with pegs or bumps. PDMS microposts with a circular base the size of a well's circumference would be glued at at the bottom of the well. The pegged base would move up and down, pushing on the PDMS and causing the microposts to deflect and induce strain in the tissue. This design can be seen below in Figure ES2.

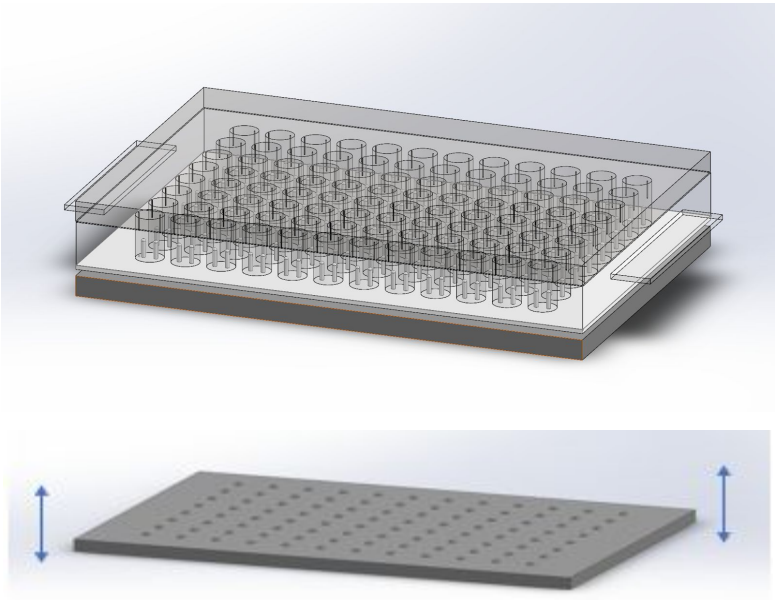

Figure ES2. Wells and pegged base.

Pronged Roller

The design is also composed of a 96 well plate but with a rotating pronged rod. As the rod rotates, the prongs are brushed against the bottom of the PDMS base, pushing apart the posts to stretch the tissue. The parts of this apparatus can be seen below in Figure ES3.

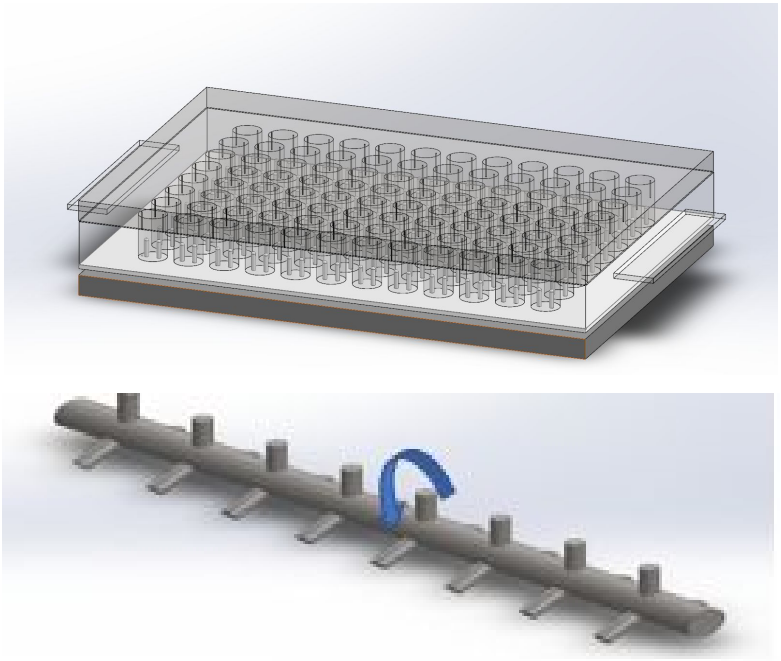

Figure ES3. Pronged Roller.

Nitinol Wires

The device is composed of a 6-well plate with two thick PDMS posts at opposite ends of each well. A nitinol wire is tied around each PDMS post and connected to a stainless steel post outside of the well. Heat is provided to the stainless steel post and conducted to the nitinol wire which then will shrink in response to the heat and therefore pulls on the PDMS posts. This will cause a deflection of the PDMS posts and produce strain in the tissue. A diagram of this apparatus can be seen in Figure ES4 below.

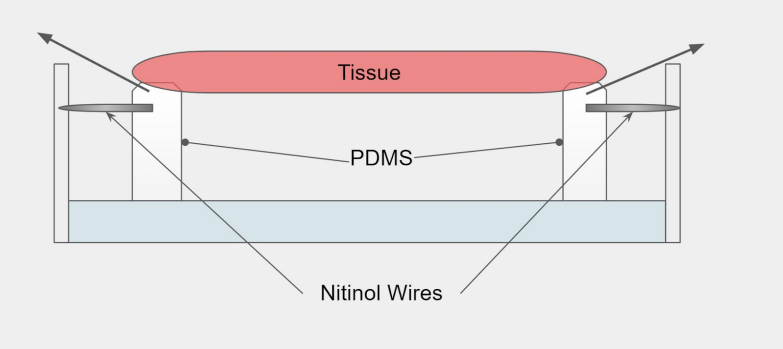

Figure ES4. Nitinol wire apparatus.

III. Final Design

The final design has 3 main components: The 3D-printed parts, the PDMS slab and microposts and the electrical components.

3D-printed Parts

The 3D-printed parts, shown in Figure 5 below, are made with biocompatible Dental LT Resin and include an air chamber, a bottomless 8-well plate and a lid. The air chamber has holes for the wires and pressure tube. The wells are oval-shaped to accommodate the shape of the tissue. The lid has a hole that is obstructed by a rubber stopper through which the electrodes are introduced. SolidWorks models of all these parts can be seen in Figure ES5 below.

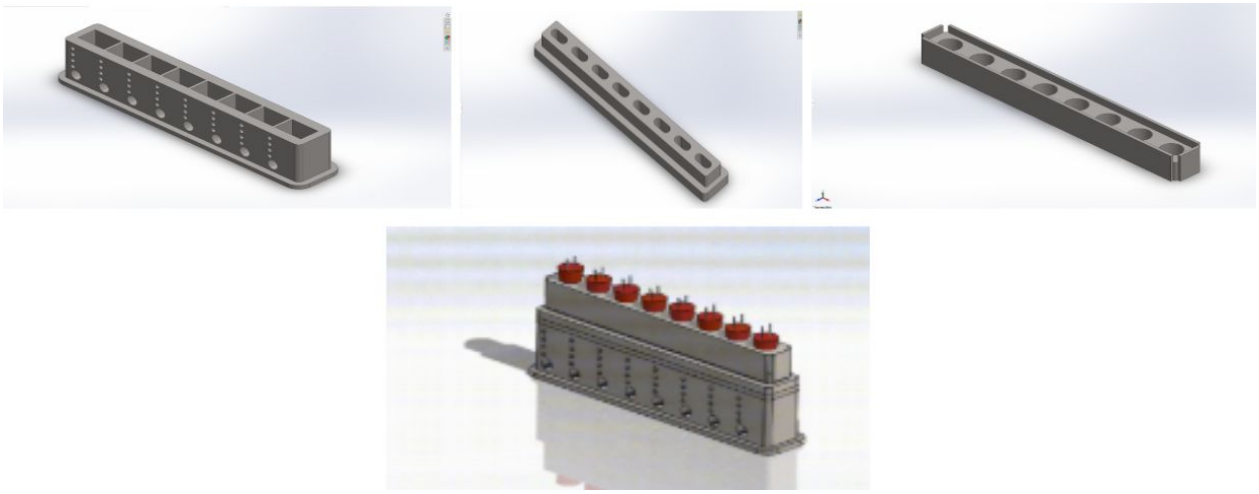

Figure ES5. 3D-printed parts. A) Air chamber base. B) 8-well plate well. C) Lid (upside-down). D) Assembled parts.

The PDMS slab and microposts

The PDMS microposts were made with a ratio of 10:1 silicon elastomer and curing agent, put in molds and cured in a Myonics Inc. Binder Oven for 30 minutes at 130℃. The slab was made with the same ratio and the Microposts were carefully aligned and cured at room temperature. The result can be seen in Figure ES6 below.

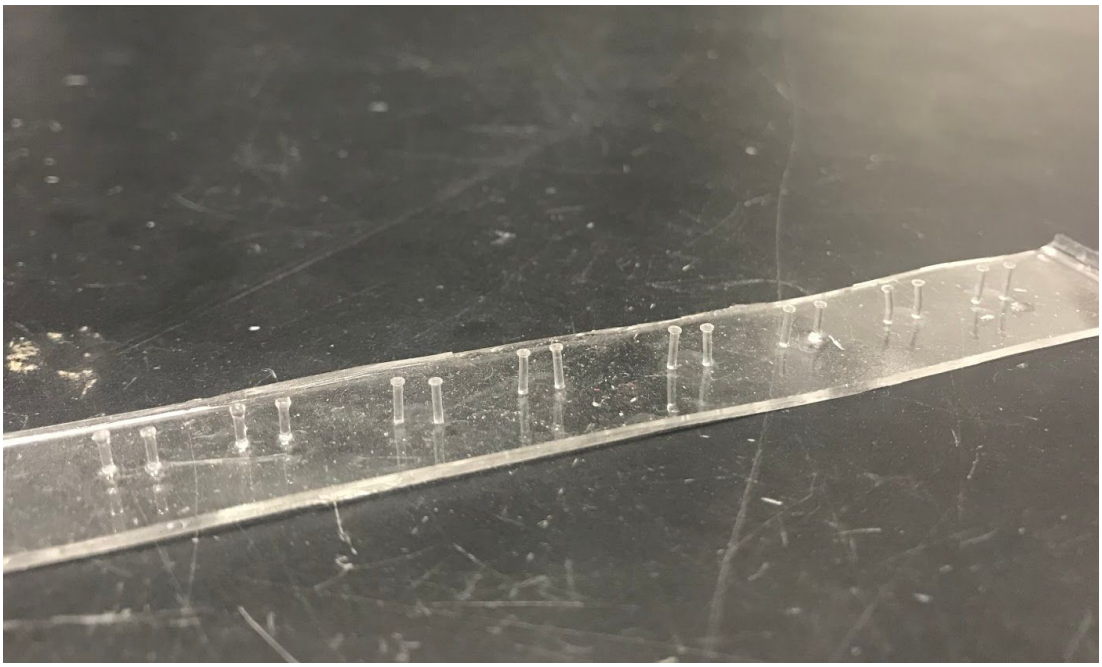

Figure ES6. PDMS slab and microposts.

Electrical Components

The electrical components include an Arduino Nano, 8 BMP280 pressure sensors, 8 pressure pumps, and 8 electrodes. The code for these items was programmed in Arduino, a C++ variant. A picture of the circuit is shown in Figure ES7 below.

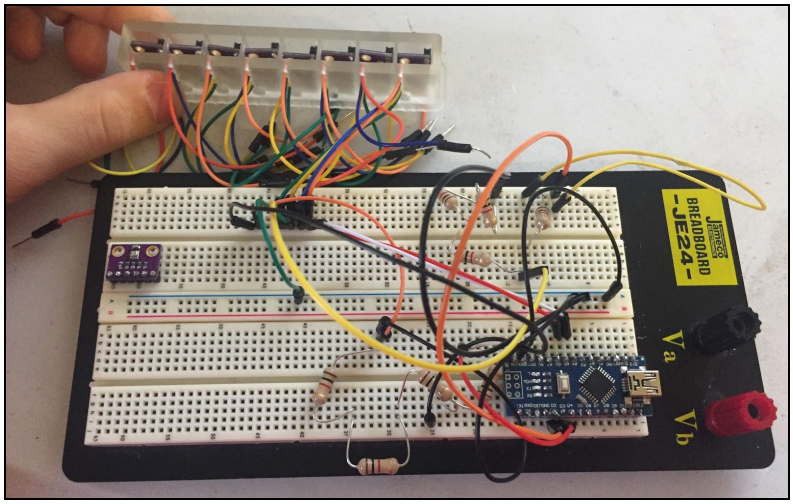

Figure ES7. Electrical components of device.

Final Design

Figure ES8 below shows a full picture of the final design with all the components assembled. This includes the 3D printed device with rubber stoppers and needles, the air pump, and the Arduino board with wires.

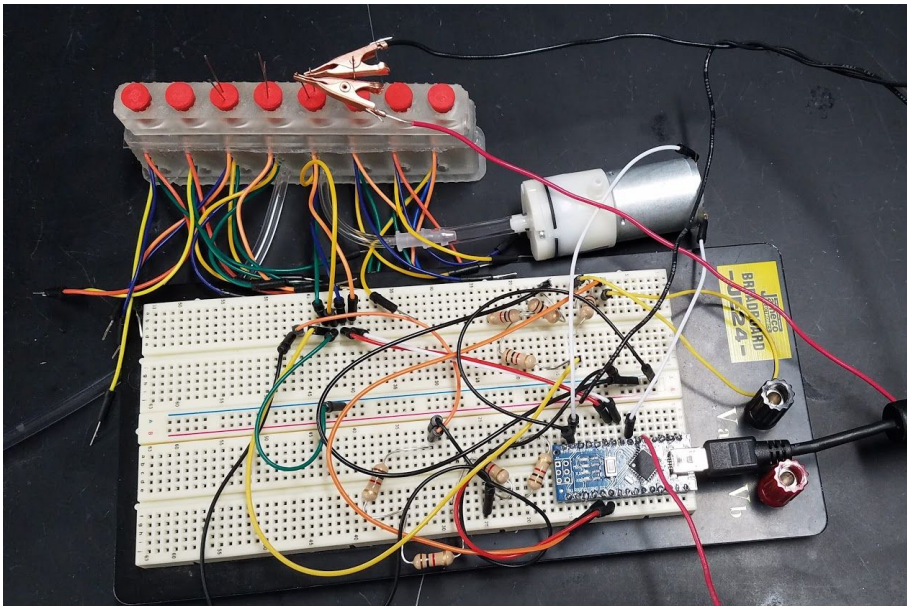

Figure ES8. Final design.

IV. Results and Discussion

Mechanical Stimulation

The device provides mechanical stimulation to the tissue by deflection of the PDMS microposts. The Arduino board provides 5V of power to pressure pumps in the air chamber which produce 20-30 kPa of pressure. This pushes up on the PDMS slab and causes the microposts to outwardly deflect. The BMP280 pressure sensors then recorded the pressure data at a frequency of 0.5 Hz. The deflection was measured at different voltages (9V, 5V, 0V) and the strain percentage were plotted as a function of pressure as seen below in Figure ES9.

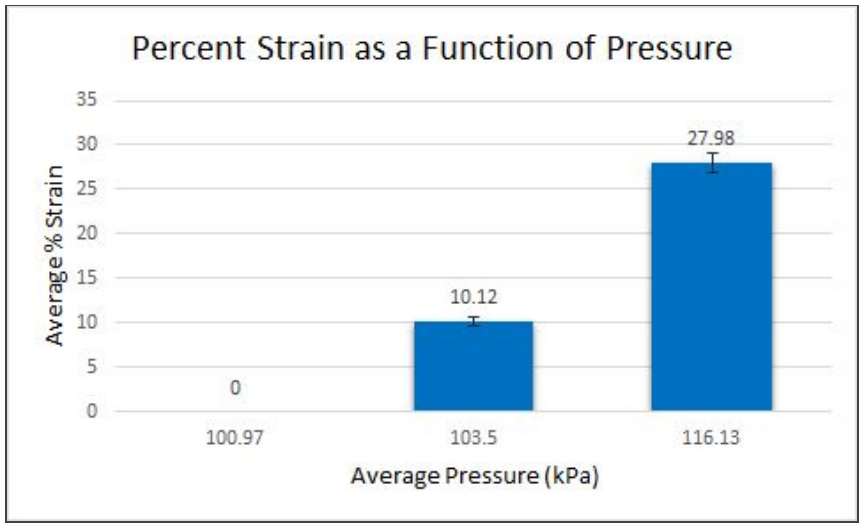

Figure ES9. Percent Strain as a Function of Pressure.

Electrical Stimulation

The wells were filled with 160 µL of complete media and electrodes were inserted through the rubber stoppers. A power of 5V was supplied to the media and the resistance measured by by fluctuated between 90 kΩ and 300 kΩ. The actual resistance could not be measured due to the constant fluctuations. The multimeter used was probably the cause of the problem. It was not well suited to measure the current resistance in liquids.

Biocompatibility Test

The device was sterilized with 70% Ethanol. Forty thousand cells were plated in each well and incubated for 3 days. The cells were subcultured and counted on the fourth day. The average number of cells in each well was found to be 21,094 cells. More than 50% of the originally seeded cells survived. This suggests that our device is not cytotoxic. The decrease in population was most likely due to the small volume available for the number of cells plated, the timespan of the test and the poor adhesion of the cells to PDMS.

V. Conclusions and Recommendations

In conclusion, the objectives were met as the device was biocompatible and with the successful post deflection, shows potential for mechanical stimulation of muscle tissue. With some improvements on the reading methods, the electrical stimulation should produce successful results as well. For 3D printing, it is important to verify all the dimensions before sending the order. It is very crucial to account for tolerance and errors.

Some recommendations include simultaneously keeping at least two plates of cell lines. This would prove useful in case unexpected issues such as contaminations were to occur. To avoid imaging issues, the well plate should not be permanently fixed to the pressure chamber. That way, it can be removed for the cells to be imaged.While making the PDMS parts, it can be hard to align the microposts. Drawing an alignment map and gluing it to the bottom of the container in which the PDMS slab is cured can be helpful. During the electrical stimulation, the electrodes experienced corrosion. To avoid this, it is important to use non-corrosive electrodes and to use a multimeter that is specifically meant for liquids. For the Arduino code, using SPI rather than I2C would make routing multiple sensors to one arduino simpler as there were only 2 distinct addresses for I2C, this required a unique configuration to use multiple sensors. Furthermore, rather than focusing on getting one component working for all the wells, it would be more fruitful to complete every feature for one well, and then expand it one well at a time until all wells were functional.

References

[1] T. Vos *et al.*, "Global, regional, and national incidence, prevalence, and years lived with disability for 328 diseases and injuries for 195 countries, 1990–2016: a systematic analysis for the Global Burden of Disease Study 2016," *The Lancet*, vol. 390, no. 10100, pp. 1211–1259, Sep. 2017.

[2]. "Myotonic dystrophy type 1 | Genetic and Rare Diseases Information Center (GARD) – an NCATS Program." [Online]. Available: https://rarediseases.info.nih.gov/diseases/8310/myotonic-dystrophy-type-1.

[3] "How many people are affected by or are at risk of muscular dystrophy?," *http://www.nichd.nih.gov/*. [Online]. Available: http://www.nichd.nih.gov/health/topics/musculardys/conditioninfo/risk.

[4] "Duchenne Muscular Dystrophy (DMD)," *Muscular Dystrophy Association*, 17-Nov-2017. [Online]. Available: https://www.mda.org/disease/duchenne-muscular-dystrophy.

[5] J. D. Walston, "Sarcopenia in older adults," *Curr Opin Rheumatol*, vol. 24, no. 6, pp. 623–627, Nov. 2012.

[6] P. Burlina, S. Billings, N. Joshi, and J. Albayda, "Automated diagnosis of myositis from muscle ultrasound: Exploring the use of machine learning and deep learning methods," *PLOS ONE*, vol. 12, no. 8, p. e0184059, Aug. 2017.

[7] DonSeiffert, "Report suggests drug-approval rate now just 1-in-10," *Amplion*, [Online]. Available: https://www.amplion.com/inthenews/report-suggests-drug-approval-rate-now-just-1-in-10.

[8] S. Caddeo, M. Boffito, and S. Sartori, "Tissue Engineering Approaches in the Design of Healthy and Pathological I*n Vitro* Tissue Models," *Front Bioeng Biotechnol*, vol. 5, Jul. 2017.

Table of Contents

Authorship

Chapters	Authors	Editors
1	All	All
2	All	All
3	All	All
4	All	All
5	All	All
6	All	All

Table of Figures

Table of Tables

Chapter 1: Introduction

1.7 billion people worldwide suffer from various muscle diseases [1]. Diseases such as Type 1 Myotonic Dystrophy, and Duchenne muscle dystrophy are genetic disorders that cause muscle wasting and can prove fatal [2,3,4]. Sarcopenia, the gradual loss of muscle tissue, is caused by aging, and as such will eventually affect everyone [5]. Polymyositis has no known cause, but has characteristics of an autoimmune disease, causing inflammation and weakness of skeletal muscles [6]. In America alone, musculoskeletal disorders cost an estimated 45 to 54 billion dollars a year in terms of lost productivity [7].

There is a need for new and improved medicines to treat these diseases. However, 90% of new investigational drugs fail phase 2 clinical trials due to lack of efficacy [8]. This represents a massive waste of time and resources that could be reduced with the ability to safely and reliably test the drugs on tissue beforehand. Existing methods for this have several drawbacks. The usage of animal tissues is flawed because animals are physiologically different from humans. Donor tissue is difficult to acquire in reasonably large amounts. Due to the high number of variables, samples would be from different donors with many known and unknown lifestyle and genetic attributes, making it difficult to determine statistically significant findings.

This leaves lab-grown tissue, or tissue engineered skeletal muscle (TESM), as the best candidate for mass-production of experimental tissue. However, this method also has limitations because TESMs are difficult to grow and the final product does not have the same characteristics as native human skeletal muscle. These include inadequate fiber diameter, limited force capacitance, and lack of migration of nuclei [9]. Without the correct mechanical and electrical stimulation TESMs do not mature properly.

The overarching goal of this project is to properly mature 3D TESMs, *in vitro*, to accurately mimic the morphologies and physiologies of a natural, *in vivo*, skeletal muscle tissue. Reaching the maturation levels of *in vivo* TESM require high contractile force generation, enlarged myofiber diameter, and the successive migration of myoblast nuclei. Accomplishing the maturation levels desired involves culturing cells in optimal conditions and the construction of a device that will provide the exercise (electrical and mechanical stimulation) to the grown tissues. To optimize efficiency, a goal of this device is to deliver electrical contractive stimulation and mechanical strain to multiple tissues simultaneously. Once the TESMs are fully mature, the final step to advancing our goal is creating disease models and subjecting our models to drugs that have known muscular effects. We then can monitor the recovery. Our goal of replicating the dynamic properties of adult skeletal muscle to TESM provides a working platform for drug screenings.

After studying the requirements of designing such a construct, we opted for with a four-step approach. The first step will consist of successfully growing myoblast monolayers over a 3-4-week period to familiarize with the cells' behavior, including growth and differentiation rates. The team will also determine the appropriate type and amounts of media contents to produce the desired behavior. The second step will consist of designing, based on literature reviews and further examinations, a multi-well construct to efficaciously grow matured 3D TESMs. The team will do extensive research on natural and synthetic biomaterials properties (compliance, toxicity, biodegradability, etc.) to identify the most suitable scaffold material for this application. Thirdly, the team will devise a method to produce mechanical stimulation in the growing tissues to induce maturation. Electrical stimulation will also be induced following currently used methods, but will not be an area of focus in this project. Maturation assessment methods will be selected from the literature.

Chapter 2: Literature Review

2.1 Clinical Significance

Between 20 and 33 percent of humans suffer from some form of musculoskeletal disorder [1]. Type 1 Myotonic Dystrophy is a genetic disorder caused by a mutation in the DMPK gene that affects roughly 1 in 8000 adults worldwide and causes debilitating muscle wasting and stiffness that can eventually prove fatal [3,10]. The muscle wasting specifically targets the lower legs, hands, neck, and face, causing difficulty walking, handling objects, making facial expressions and eating or drinking [10]. Polymyositis has no known cause, but has the characteristics of an autoimmune disease in which the immune system attacks the body. It is an inflammatory myopathy, chiefly characterized by chronic muscle inflammation and weakness, mostly targeting skeletal muscles [11]. Duchenne muscle dystrophy is an x-linked recessive genetic disorder that causes progressively worse wasting of skeletal muscles and the heart. Symptoms appear early in childhood, and the disease mostly affects males, although it can rarely appear in females [12]. Even with recent advances in medical technologies extending average life spans, the life expectancy of people with Duchenne muscle dystrophy only reaches the mid 30s [13]. Sarcopenia is the muscle wasting caused by aging, and as such will eventually affect everyone, with symptoms beginning to manifest as early as the 4th decade of life, and with half of the original skeletal muscle having wasted away by the 8th [14]. These kinds of diseases have a severe impact not only on those who suffer from them, but also on the economy. In America alone, musculoskeletal disorders cost an estimated 45 to 54 billion dollars a year in terms of lost productivity [7].

There is a need for new and improved medicines to treat musculoskeletal diseases. However, the process of creating new medicines and treatments is lengthy, expensive, and prone to failure, with only about 9.6% of potential treatments passing all phases of clinical trials and gaining FDA approval for marketing [8]. Phase I clinical trials involve exposing healthy adults to the drug in various quantities, to test the drug for its basic properties and risk of toxicity. Phase II clinical trials involve testing the drug on people suffering from one or more conditions the drug is supposed to treat, and comparing the impact the drug has to the impact of industry standard treatments and untreated patients. Phase III trials test for both safety and efficacy, but involve many more subjects than the previous two phases, potentially thousands of people or more [15].

The failure rate of new drugs in clinical trials could be greatly reduced with the ability to test them on human tissue beforehand, in the form of engineered tissues grown outside of the body. If there were a method to allow for the testing of drugs on mature tissue prior to clinical trials

involving animals and humans, unexpectedly toxic and ineffective drugs could be filtered out before clinical trials even began. The removal of these drugs which would eventually be found ineffective would result in less wasted time and resources, allowing for more effective drugs to make it to market faster.

2.2 Skeletal Muscle Physiology

To understand the clinical significance of the the project and be able to compare TESMs, the expertise of physiologies behind native human skeletal muscle is necessary. The adult human body is composed of over 640 muscles, which account for an average of 42% of body mass for males and 36% of body mass for females [16]. This system makes up such a huge part of the body because it plays a critical role in every aspect of daily life. This chapter outlines the basic functions, composition, and the process of contractions of the skeletal muscle system.

2.2.1 Functions

The skeletal muscle has many functions, but the most notable is its ability to contract to produce movement. It can also resist gravity to maintain posture. The skeletal muscle is connected to the bones via tendons, which keeps joints stable as they can become misaligned when pulling on the corresponding bone. This also stops excess movement in the bones and joints, protecting the skeleton from structural deformation. Because the skeletal muscle system eccompasses most of the body, it is providing an external barrier to protect internal organs, especially abdominal and pelvic organs. Besides from contributing to the structural integrity of the body, this organ maintains the body's homeostasis by generating heat during contractions. For example, in the cold the body involuntarily produce contractions known as shivers, to generate heat. As seen, any chronic or major deterioration to a muscle will hinder these important functions and impair basic daily activities [17].

2.2.2 Structural Hierarchy

Bundles of myofibers are grouped into compartments separated by layers to form a whole muscle and can be structural compared to that of a rope, in which groups of strands are bundled together and bundled again to form a long strong sturdy product. The structural breakdown of a muscle can be seen in Figure 1 below.

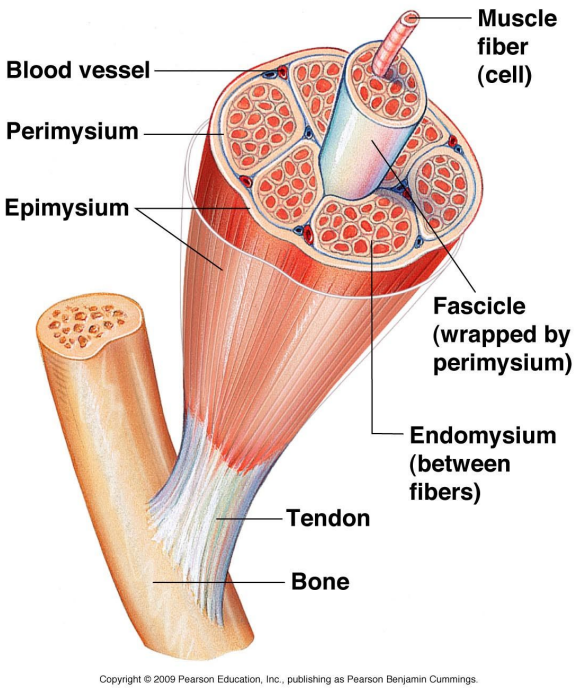

Figure 1. Skeletal muscle structure.

Starting from the outside in, the fascia surrounds each muscle in the body and they project inward, separating each muscle. Underneath reveals three extracellular matrix (ECM), composing of the epimysium (around the muscles), the perimysium (around the fascicles), and the endomysium (around a muscle cell). These ECM play important roles in muscle functions, such as adaptability and regeneration, by providing a scaffold for structural support for cells to attach and proliferate. They are composed of majorly different types of collagen, proteoglycans and glycosaminoglycans, and glycoproteins [18]. Each muscle is surrounded by the epimysium and is composed of fascicles. These fascicles are surrounded by the perimysium and house muscle cells. These muscle cells are surrounded by the sarcolemma and are made of myofibrils as seen below in Figure 2.

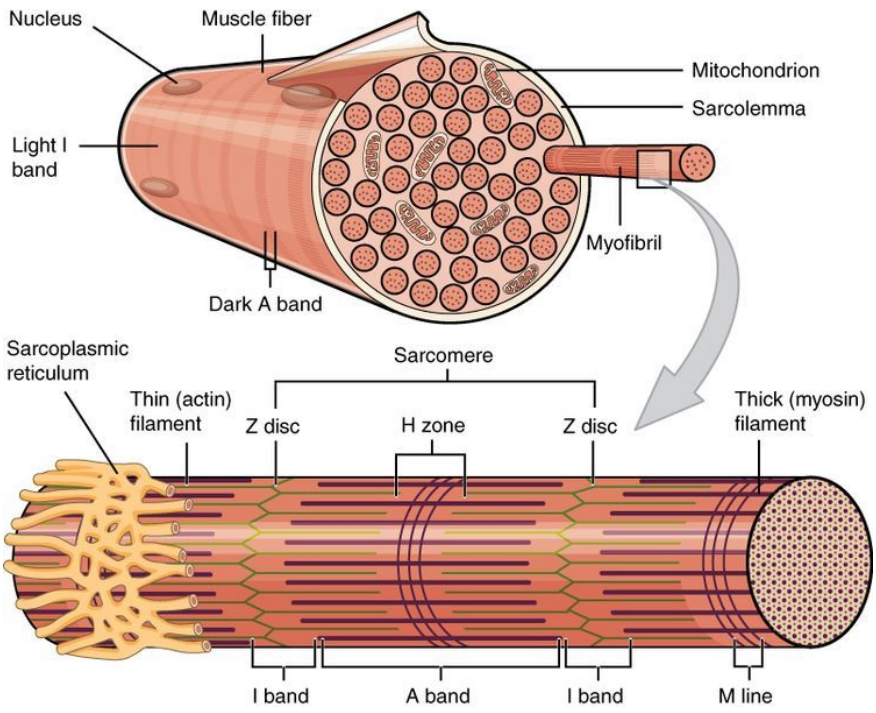

Figure 2. Structure of a muscle fiber [18].

Each myofiber (10-100 micrometers) are hundreds of fused myoblasts and runs the entire length of the muscle from one end to the other. The nuclei of each myoblast can be seen underneath the sarcolemma in Figure 2. The myofibrils are surrounded by their own special network of sarcoplasmic reticulum (SR) containing rich calcium ions. Myofibrils are made up of the actin-myosin protein apparatus and T-Tubules, both play important roles in producing movement. Actin are thin filaments anchored to the Z-line and can be found in I bands, whereas, myosin are thick filaments centered around the M line and are found in the A band. Myofibrils are divided into subunits call sarcomeres. The ends of each sarcomere are called Z-discs [19]. Understanding the molecular structure is essential for maturation assessment of TESMs.

2.2.3 Contraction Process

The skeletal muscle is known for producing motion and this occurs through many microscopic processes also known as the sliding filament model. First, the brain sends an action potential along the motor neuron until it reaches the synapse of the muscle cells and continue throughout the sarcolemma membrane. An action potential is the temporary depolarization of a motor neuron in order to send a signal down the neuron and is caused by sodium flooding into the neuron due to voltage-gated channels opening. These action potentials only last about 2 ms before the neuron repolarizes to reset its normal potential [20]. The motor neurons then release acetylcholine into the synapses, opening sodium channels. The depolarization of sodium and potassium reach T-Tubules, triggers the voltage sensitive protein connected to the calcium

channels in the SR, and cause the release of calcium ions into the cell. Figure 3 below shows the full cycle of ions.

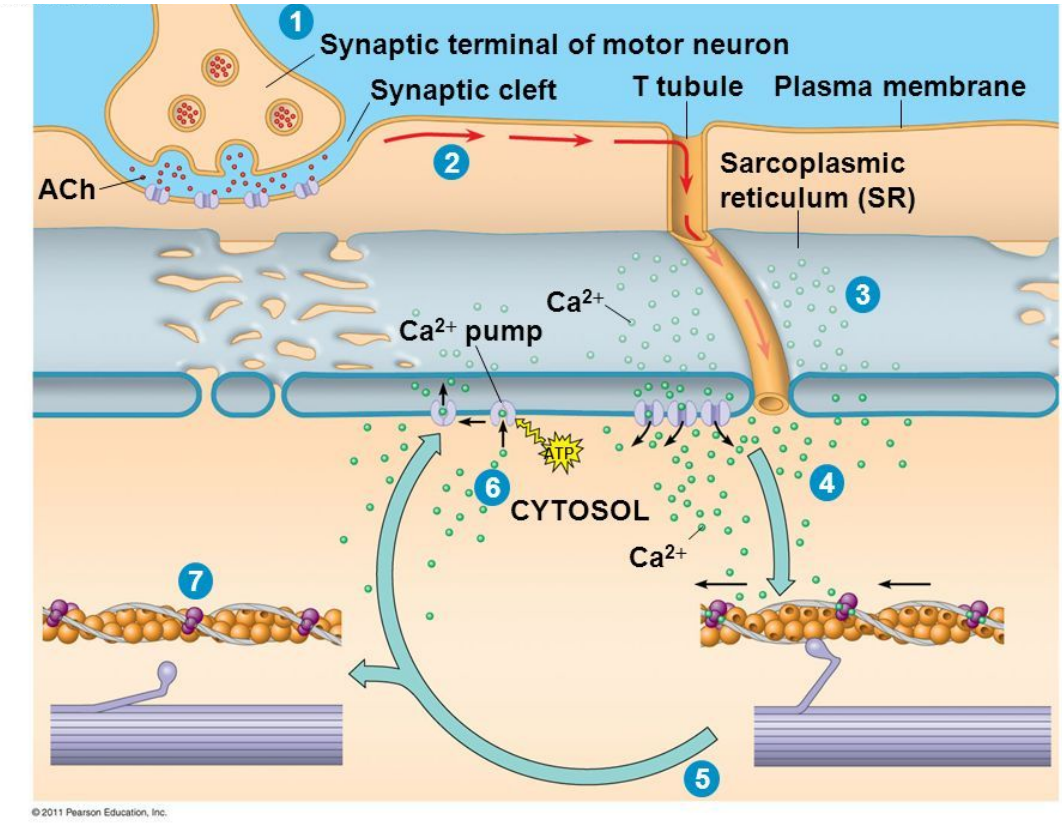

Figure 3. Mechanism of contraction action [19].

The main players in the movement of the muscle are the proteins actin and myosin. The binding of these two proteins cause shortening of a sarcomere, pulling the muscle fiber together to produce a contraction. However, the troponin and tropomyosin, protein bodyguards, covers the binding site on the actin during rest. During contraction, the calcium that is released from the SR will bind to the troponin causing the tropomyosin to move and expose the binding site. An illustration of the activated actin and myosin can be seen below in Figure 4 [21]. Myosin uses energy by breaking down ATP to ADP and a phosphate. The myosin will move into an extended position like a stretched spring preparing for its powerstroke. Finally, it releases the stored energy to bind to the actin site and pulling the strand the other way to shrink the sarcomere. Millions of actin and myosin slide over each other simultaneously to produce contractions in a whole muscle. The cycle continues, in which the myosin goes back to its resting phase when the ADP/phosphate unbinds and a new ATP binds to change back the actin's shape. Calcium is needed to restock the SR so they unbind from the troponin, which also cause a change of shape in the tropomyosin, covering the binding site. The muscle relaxes and the whole cycle repeats again.

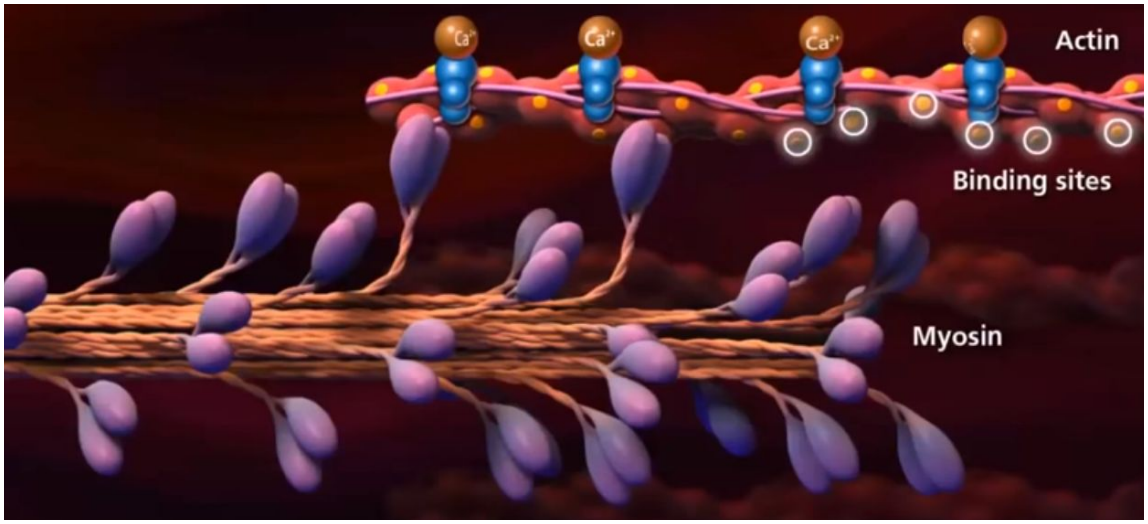

Figure 4. Activated actin and myosin fibrils [21].

For the mechanism of contraction to occur, the three main requirements are: there must be a neural stimulus, availability of ATP, and presence of calcium within the cells. A contraction is stopped when the nervous system cannot produce enough impulse to trigger the release of calcium ions, there is no more ATP causing fatigue of energy, or the sensory neuron will inform the brain when an injury occurs. Any of these continuous disruptions will hinder the muscle's contraction ability and lead to the deterioration of the muscle strength. Additionally, because action potentials can only alter the process of depolarization and repolarization, continuous muscle contraction is a function of the repeated activations of the muscle before it can relax. This is called summation and is used by the body for graded responses to stimuli. If the muscle is stimulated within 20-50 ms of the initial stimulation, then the muscle will contract further than the initial contraction [22]. However, repeated muscle contractions builds up lactic acid, which interferes with the body's ability to generate and use ATP. This means that the myosin no longer can effectively bind to and move the actin fibrils, and so the muscle slowly starts to lose the ability to contract properly. This event is called fatigue, and in healthy adult muscles it allows for a recovery period to strengthen the muscle [22].

2.2.4 Embryonic Myogenesis

Muscle formation initializes during the embryonic life in the paraxial mesoderm, which are segmented into somites. Somites are epithelial structures forming at day 20. These are divided further into the ventral portion sclerotome, dorsal portion dermatome and myotome. Sclerotome forms vertebrae, dermatome forms the derm, and myotome forming skeletal muscles. After somites differentiate to myotomes, specification to myoblasts starts in the c-Met-HGF pathway when muscle progenitor cells are recruited by mesenchymal cells. The specification occurs through signaling molecules, such as, Sonic Hedgehog and Wnt proteins. After specification, the

myoblasts divide and migrate to their differentiation destination with the help of transcription factors. Then, these myoblasts undergo two myogenesis, successive waves of fusion, to form myotubes and finally to a multinucleated muscle fiber. The last step is the formation of quiescent myoblasts, satellite stem cells, that are found between the connective tissue basement membrane and the sarcolemma and are essential to muscle regeneration. The embryonic myogenesis process is displayed in Figure 5 below [23].

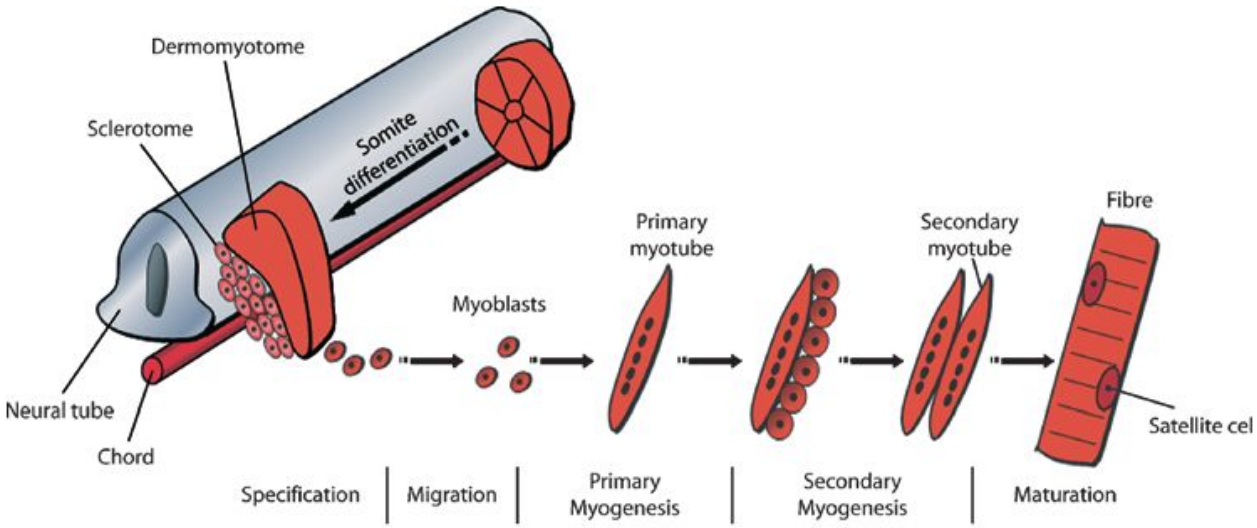

Figure 5. Muscle development in the embryo [23].

2.2.5 Tissue Regeneration

Injuries to the skeletal muscle are common throughout life and the skeletal muscle has robust regenerative properties, allowing muscles to recover completely if the injury did not cause more than 20% of volumetric loss [24]. With minor injuries, such as, a strain or tear in the muscle due to strenuous activity, nearby satellite stem cells residing on top of the sarcolemma will activate. They divide and differentiate to produce daughter myoblasts that fuse into the injury site of the myofiber. The mother myoblast will renew back into its original stem cell state for future repair. With major trauma of more than 20% volumetric muscle loss, the muscle will undergo three phases displayed in Figure 6 below [24].

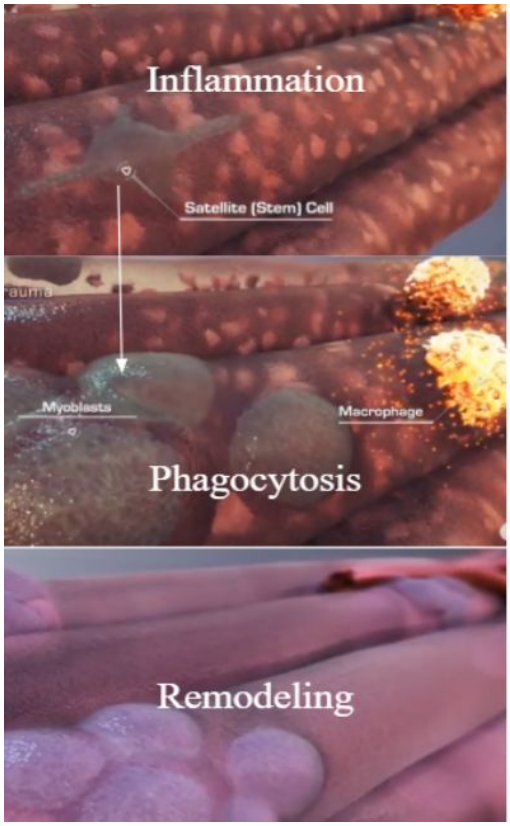

Figure 6. Phases of muscle regeneration [24].

The first phase is the inflammatory response, in which cell necrosis occurs. The ruptured myofiber release proteases that quickly break down damaged fiber. To contain these proteases from degrading undamaged fibers, a contraction band of cytoskeletal components surround the damaged fiber. The proteases along with other cellular signals recruit macrophages, initiating phagocytosis and clearing away residual damage debris. They interact with satellite cells to speed up chemotaxis. After 24 hours, a second wave of macrophages secret anti-inflammatory factors to promote tissue regeneration. The last stage is the remodeling stage, in which satellite cells activate, proliferate and fuse to form new muscle fibers. Fibroblasts also release collagen and EMC protein, fibrin, to form scar tissue and clot to stop the bleeding. The muscle fiber reorganizes and restores function back to the muscle [24].

2.2.6 Mechanical Properties of Native Skeletal Tissue

During contraction, muscle tissue exerts a force on the skeleton to move it. This contraction force is maximum when the muscle is at 33% strain, meaning the muscle exerts the most force when it's at 1.33 times its resting length [25]. The contractile force generated by in vivo skeletal tissue varies greatly between muscle groups and individuals. It is considered a function of the length of the muscle and its cross section, which more appropriately estimates the number and thickness of

the myofibers in the muscle. As the length and the cross area of a muscle increases, the potential contractile force also rises [25]. The quadriceps are one of the largest muscle groups and are weight bearing; they can voluntarily exert a contractile force (N/kg) equal to 75% of the person's body weight. Under electrical stimulation, the quadriceps can exert a contractile force (N/kg) equal to 60% of the person's body weight [26]. This means that the quadriceps of an average woman weighing 168.5 lbs (76.4 kg) can exert up to 57.3 N of contractile force [27]. The contractile strength of the gastrocnemius, however, is much smaller. The average woman's gastrocnemius can produce a contractile force of up to 29.4 N [28,29].

2.3. Current Practices and Limitations

Currently, there are multiple techniques that allow for testing of drugs prior to clinical trials, but there are multiple limitations to each method.

2.3.1. Animal Models

Animal models are easily acquired in large numbers and can be used to simulate a full body system. That being said, as they are not humans, they have different anatomies and physiologies from humans. Furthermore, human-like animals tend to be more expensive and difficult to acquire. The cost of using large numbers of animals can also rise quickly, especially if the animals must be replaced often - the cost of buying, feeding, and housing a lab rat can be around ten dollars a week, and large experiments would need dozens if not hundreds of rats over the course of months, costing hundreds of thousands of dollars to experiment on animals that do not accurately replicate the human body [30].

2.3.2 Donor Tissue

Donor muscle tissue is difficult to acquire in large amounts. This is because removing any significant amount from a healthy human could cause permanent damage and it would require many people to donate to obtain a usable amount for testing. Testing on tissue with a known musculoskeletal disorder exacerbates this problem, as people suffering from the diseases are usually not able to safely donate muscle tissue. Additionally, there are countless variables inherent to donor tissue, related to the family history and lifestyle of the donor, many of which cannot be known to experiment conductors and none of which can be adequately controlled. The lack of variable control makes it difficult to produce conclusive findings, as there could be many unknown factors influencing the results.

2.3.3 *In Vitro* Skeletal Muscle

Two-Dimensional Muscle Tissue

To supply the need for engineered skeletal muscle tissue, it is important to recreate tissue models that mimic natural tissues as accurately as possible. To achieve this goal, researchers have used different techniques to grow monolayer (2D) tissues for preliminary drug testing. One method consists of growing tissues on 2D micropatterned surfaces with periodic features (from a few nanometers to less than 100 micrometers) [31]. The 2D micropatterned surfaces allow for a guided alignment of muscle myoblasts and myotubes from fusion of myoblasts and lead to formation of pre-patterned cell sheets. However, cell sheets grown on these micropatterned surfaces have very limited thickness. Another widely known drawback of 2D tissues is that they lack many phenotypic characteristics of *in vivo* tissues (thickness, contractile force, cell-cell interactions, etc.), making them unfit for drug assays [9].

Three-Dimensional Muscle Tissue Without Stimulation

In order to produce more accurate tissue models, researchers have opted for engineered 3D skeletal muscle tissues. 3D models for drug testing offer many advantages over animal and 2D models [9]. These advantages include the ability to have cell to cell and extracellular matrix (ECM) interactions in all the spatial dimension. 3D tissues can be made using a 3D matrix (scaffold) or scaffold-free organoids cultures. Organoids allow for drug efficacy and side effects testing [32]. Although organoids would be a better option than 2D cultures, scaffold-based tissues show even more success in drug testing applications because are able to assist proliferation, differentiation, and biosynthesis of cells [33]. Methods to produce skeletal muscle tissue include 3D scaffolds with aligned pores, mesoscopic hydrogel molding and stacking of aligned tissue sheets [34]. The biggest challenge in growing 3D tissue is to properly stimulate them. Electrically stimulated myotubes show increased fusion and retain their contractile ability for a longer period of time [35]. Although 3D matrices provide support that mimics in vivo and incorporate growth factors, some of their drawbacks include the high cost for large-scale production and the deficient distribution of nutrients throughout the construct [36].

Biomaterials for Scaffolds

Finding the right material to make scaffolds for a specific application is another challenge. The ideal biomaterial for scaffold applications should be bioresorbable. It should allow the engineered tissue to maintain sufficient mechanical integrity to support itself in early development and by the time the tissue matures, it should have started degrading so that it cease tissue growth. There are 3 classes of materials commonly used for scaffold production: naturally derived (e.g. alginate, collagen), acellular tissue matrices (e. g. bladder submucosa, small intestinal submucosa) and synthetic polymers (e.g. polyglycolic acid (PGA), polylactic acid

(PLA), poly (lactic-co-glycolic acid) (PLGA)) [37]. Alginate, collagen, fibrin and other naturally derived materials use to develop hydrogels for 3D tissue scaffolds are porous and to incorporate ECM molecules that communicate *in vivo*-like signals to cells and enables them to show *in vivo*-like cell behavior [36]. Their pore sizes can be manipulated as necessary during production making them a good candidate for engineered tissue. The advantage of natural compounds is that they are more likely to be biocompatible and nontoxic. However, synthetic polymers offer the possibility of large-scale reproducibility of important mechanical properties such as strength, degradation rate and microstructure

Apart from biocompatibility, non-toxicity, biodegradability and mechanical properties, another important requirement for a good scaffold is porosity. It should have interconnected micropores, so that cells can be seeded and be able to migrate into the inside of the scaffold. Micropores are crucial for vascular formation and waste transport, without which cells would not survive. An optimal pore size is in the range between 100 and 500 μm [33].

Different scaffolds can highly affect the maturation of the tissue. Cells are able to sense the stiffness of the ECM and will replicate and differentiate only if provided with *in-vivo*-like conditions [34]. The properties of the matrix determine how efficiently individual muscle cell contractions integrate at the macroscopic tissue level and how externally applied mechanical stimuli transmit to individual cells.

Strategies for Advancement

A way to improve on prior methods of engineering skeletal muscle tissue is to stimulate the tissue during development. This mimics the natural conditions under which muscle grows while in the body. Electrical stimulation causes the muscle to contract, as it does when it receives signals from motor neurons in the the body. Mechanical stimulation causes the muscle to stretch, as it will when the muscle is relaxed in the body, and an opposing muscle contracts. For example, when the bicep on the front of the upper arm is stimulated by neural impulses, it contracts, causing the arm to flex. This flexion causes the tricep, on the back of the upper arm, to stretch. This project will focus mainly on mechanical stimulation during development.

Novel Stimulation Methods

Muscles need to be stimulated both mechanically and electrically. Mechanical stimulation of muscle tissue is performed by having an external mechanism apply a tensile force to the tissue. Bioartificial skeletal tissue has a wide range of recorded mechanical properties due to the variations in setup and training regimen. Though muscles are strained in vivo up to 33%, the majority of studies only strain the bioartificial tissues 10-20% [38]. This means that the bioartificial tissues are not exercised as strongly as in vivo muscle, but it also prevents the tissue from becoming saturated with oxides. In addition, bioartificial tissue under 20% strain showed a

decrease in MyoD and MNF-α concentrations compared to lower strains [38]. This means that the tissue was producing few transcription factors to differentiate the cells and create myofibrils. However, satellite cells have been observed to increase their proliferation at 25% strain [38].

The level of strain is important, but the type of strain can drastically change the growth of the tissue. Static strain, where the tissue is not moved and the strain results from the positioning and natural growth of the tissue itself, is the most commonly used type of strain and has been the strain discussed previously. Cyclic strain is an alternative to static strain, where the tissue is mechanically stretched in a cyclic pattern. Cyclic strain is more closely representative of the type of strain placed on muscles in vivo, but produces similarly unrepresentative results as static strain in vitro, preventing the biomedical field from conceding one as better than the other. Studies using cyclic strain have used strains of 10-60%, and have observed that oftentimes 40% strain increased myogenic factors like MyoD compared to other strain levels. However, the level of myogenic factors in the cyclic studies were still lower than in static studies [39]. Regardless of the strain, bioartificial tissues still only produce contractile forces in the milliNewtons, nowhere close to the contractile force of in vivo skeletal tissues [39].

Two of the earliest devices employing mechanical stimulation to aid in skeletal muscle tissue growth were developed by Vandenburgh et. al [40]. They were known as Mechanical Cell Stimulator Model I and Mechanical Cell Stimulator Model II. Model I, pictured in Figure 7, functioned by allowing the muscle tissue to grow without mechanical stimulation initially.

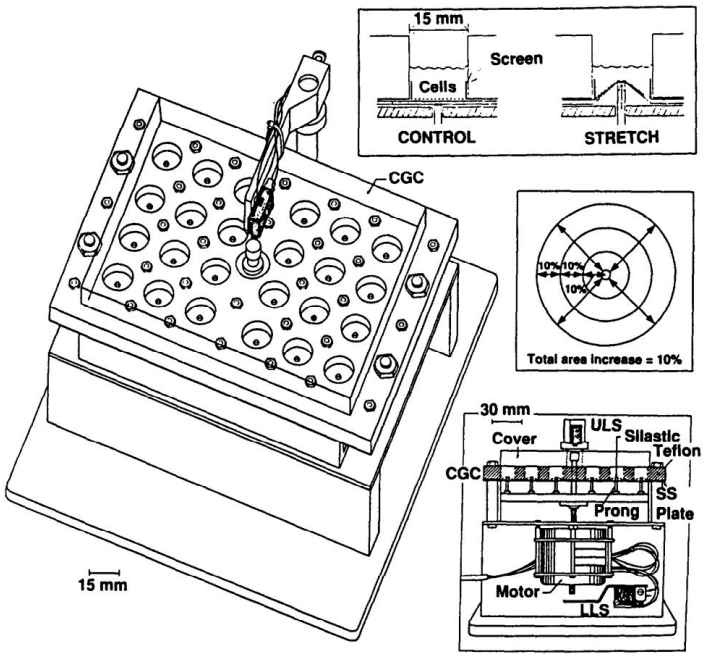

Figure 7. Mechanical Cell Stimulator Model I [33].

The tissues grow in branches and are allowed to attach to the walls of the wells encasing them. Once a certain stage of growth is reached, vertical prongs are pushed into the wells through holes in the center of the bottom of each well. These prongs then collide with and push the muscle fibers, stretching them [40]. However, the holes necessary to accommodate the prongs presents an additional risk of infection.

Mechanical Cell Stimulator Model II, pictured in Figure 8, followed a similar procedure, but stretched the muscle cells differently.

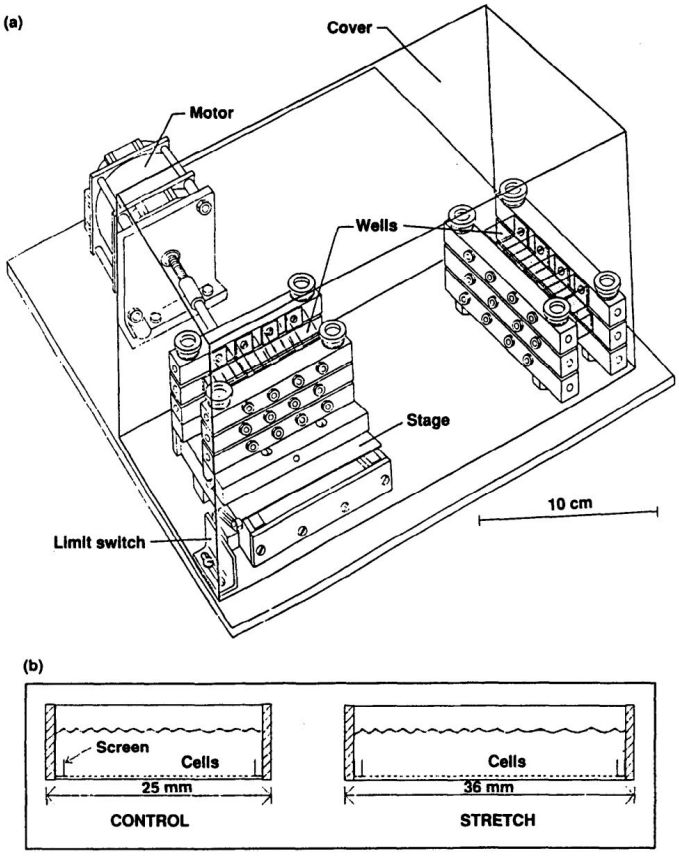

Figure 8. Mechanical Cell Stimulator Model II [40].

The wells in which the tissues are grown are now rectangular wells, as opposed to the circular wells of Model I. The motor is used to stretch the elastic wells horizontally, stretching the muscle tissue in one dimension [40]. However, this strategy would make it more difficult to accommodate electrical stimulation.

Electrical stimulation of bioengineered muscle has a similarly wide range of recorded mechanical properties as mechanical stimulation. Native skeletal tissue does not have a single electrical stimulation voltage value; the local voltage change due to the action potentials in the muscle differs depending on how many somatic neurons are firing and the density of somatic neurons in the area. Experimentally, it has been shown that bioengineered tissue develops more organized myofibrils and uniform cell layers. In addition, electrically stimulated cells developed functional sarcomeres with mitochondria between each sarcomere bundle [41].

One of the more successful experiments to utilize electrical stimulation was Hyoungshin Park et al.'s electrical stimulation of C2C12 cells. C2C12 cells are mouse myoblast cells, used often in lab experiments due to their relative ease of use and more rapid growth and differentiation rate. Park et al. cultured their C2C12 cells for 3 days, until they were roughly 85% confluent, then transferred the cells into a collagen scaffolding. A platinum wire was used to apply electrical stimulation to the cell-collagen construct for 5 days. The electrical stimulation used followed one of six regimens, using 2, 5, or 7 V at a rate of 1 or 2 Hz. When compared to the control cells, which were not stimulated, all of the stimulated cells differentiated further and organized more than the control did. The cells exercised at 5 V showed the best formation of contractile groups, both at 1 Hz and 2 Hz. Additionally, the 2 Hz groups showed less collagen when histogrammed, meaning that the cells had replaced the collagen scaffolding with functional cells [41]. However, the setup of this experiment would not be suitable for mechanical stimulation of the cells, as the collagen scaffolding would interfere with the mechanical straining of the tissue.

Chapter 3: Project Strategy

The goal of this project is to design a construct to mechanically stimulate tissue engineered skeletal muscle. In this chapter, the client statement will be evaluated through design requirements both technically and standard, and the project strategy will be discussed.

3.1 Initial Client Statement

The initial client statement was to: “Design a device that allows for reproducible 3D long-term culturing of accurately stimulated human skeletal muscle. The system should be able to measure contractile force *in situ*, and be adaptable to a multi-well/construct format that enables rapid and reproducible assessment of muscle response to various drugs and doses.” This initial statement was simplified down to: design a multi-well construct in which 3D skeletal tissue can be electrically and mechanically stimulated to form differentiated adult skeletal tissue for drug testing and disease modelling.

3.2 Design Requirements

This section lists and discusses objectives, constraints, and specifications to design and achieve proper maturation characteristics of *in vivo* human skeletal muscles.

3.2.1 Objectives

Using the client statement, the team identified main objectives. Then, literature was used to identify sub objectives or specific goals. The main objectives are:

- The design must be able to grow cells to allow for tissue formation. This means that the construct must support cell differentiation and proliferation to form tissues that can be mechanically stimulated without damage and rapid depletion of media. Once contraction occurs anchors are needed to provide stability as native human skeletal muscle are anchored on bones through the tendons.
- The characteristics of TESMs needs to replicate that of *in vivo* skeletal muscles as accurately as possible. For example, the migration of nuclei to form myofibrils and the density of these multinucleated are an essential comparison. The structure of the tissue need to have the same physical properties as native cells. This includes diameter and length size, force generation, and strength as the fiber should not tear when undergoing stresses and strain exercises. These characteristics need to be consistent throughout all wells to produce repeatable results.

- Stimulation is important for cell maturation as skeletal muscle cells in the human body are constantly subjected to forces. Mechanical stimulation work to stretch the tissue to provide a strain exercise, whereas, electrical stimulation work to contract the muscle.
- When cells are mature, they will contract to produce a force throughout their lifetime. This contractile force should be easily measurable in realtime to compare to native tissues and also test the effects of muscular drugs.
- A multi platform is needed, in which multiple tissues are growing and can be simultaneously stimulated to provide a high throughput platform to efficiently test drugs.

Figure 9 below, is a representation of the hierarchy of the main objectives and the sub objectives.

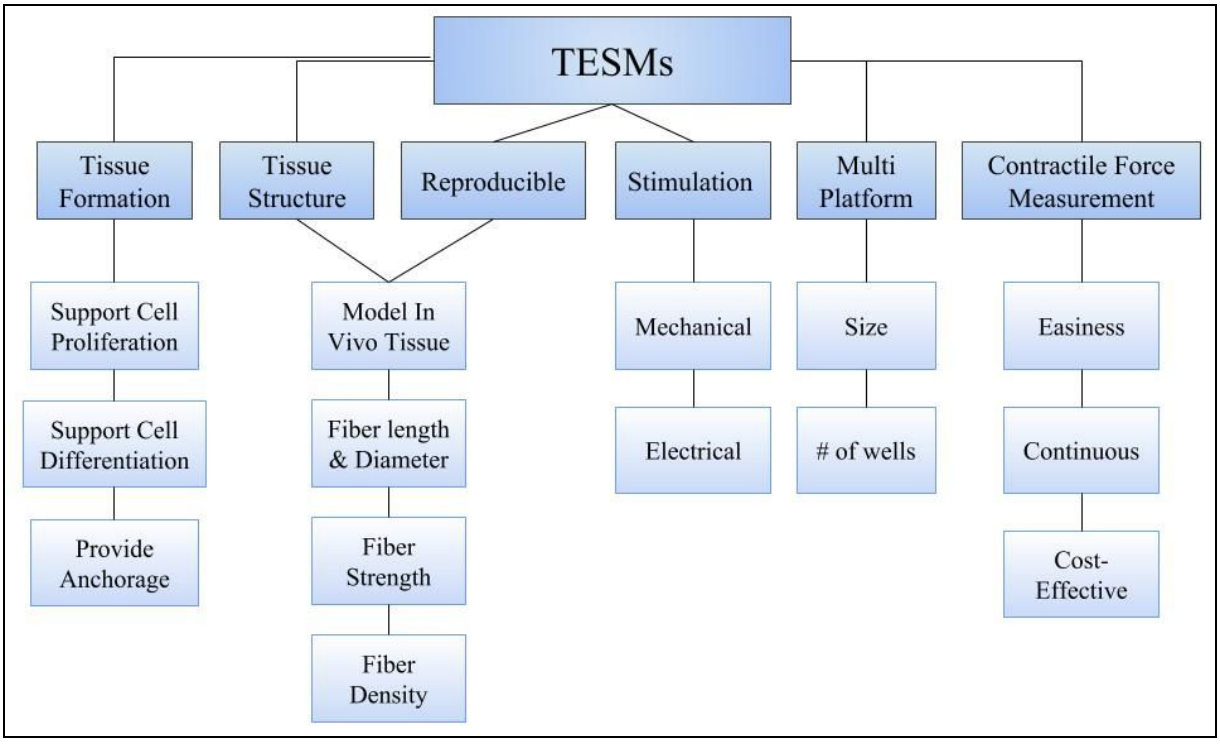

Figure 9. Objective tree.

The main objectives are then plotted against each other in a pairwise comparison chart so they can be ranked in terms of importance. This is shown in Table 1 below.

Table 1. Pairwise comparison chart of objectives.

	Tissue Formation	Tissue Structure	Stimulation	Contractile Force Measurement	Multi Platform	Score
Tissue Formation	x	.5	.5	1	1	3
Tissue Structure	.5	x	.5	1	1	3
Stimulation	1	1	x	1	1	4
Contractile Force Measurement	0	0	0	x	1	1
Multi Platform	0	0	0	0	x	0

The above pairwise comparison chart of the main objectives yield the following ranks with the highest rank as the most important to the lowest being the least important:

1. Stimulation - this is the most important objective because stimulations are essential for cell maturation and the desired tissue structure.
2. Tissue Formation and Tissue Structure - these tied because the tissue needs to form and mature before the structure can be analyzed.
3. Contractile Force Measurement - this ranked second to last because tissue needs to form to produce contractile force.
4. Multi Platform - this ranked last because if one cell does not achieve the desired maturation, then a design focusing on a multi platform is futile.

3.2.2 Constraints

The design constraints act as parameters for the design process and are listed below based on the client statement:

- Remain within budget of $750
- Design must fit in the incubator of 2’x2’x1’
- Design must withstand incubator conditions of 37°C, 5% CO_2, 95% humidity
- All mechanical parts must be sterilized and be able to sterilize
- Project needs to be completed within 21 weeks
- Any parts in direct contact with cells need to be biocompatible
- Design should utilize on campus resources or easily accessible resources
- Constraints regarding cells:
    - C2C12 are used even though they are mouse myoblast cells, this is because mesenchymal stem cells take too long to culture
    - Cells should be under confluence of 60%-70% in 2D culture

- The tissue formed should be of a diameter that does not require blood flow or vascularization

3.2.3 Functions

Multi-well construct

The device must be a multiwell construct to allow for reproducibility in the experiment. However, the team decided to initially design the stimulation device as a single-well construct to allow for a thorough study of all the specifications involved. The system will later be multiplied into a multiwell apparatus.

Growing tissue

The tissue will be grown in a rectangular mold made of PDMS or PLLA. The material will have moderate stiffness. This is to allow the mold to stretch and relax upon application of a force. The tissue will be stretched along with the mold. The tissue will be anchored to the ends of the mold using different methods discussed in the next chapter. The selected material can be submitted to an air plasma treatment to increase hydrophilicity and allow better cell growth.

Mechanical stimulation

In order for the tissue to attain maturation, it must be stimulated. The team will mechanically stimulate the tissue construct using a variety of means. Some preliminary methods include using the shape memory effect of a nitinol wire, using a magnetic field and using a force probe to stretch and contract the tissue contained in a sterile mold. More details on the designs will be discussed in the next chapter. The team will need a force transducer to record the magnitude of the force applied as the tissue is stretched. The strain will be measured through an imaging software such as ImageJ. With the ductile mold, the tissue strain can be approximated based on mold strain.

Electrical stimulation

For electrical stimulation,small electrodes will be used to induce microscale contraction in the tissue will be performed. The intensity of electric discharge and the appropriate electrode will be determined from literature and not from experiments as electrical stimulation is only a secondary objective in this project.

Sterilization

It is important to sterilize the equipment in a way that does not alter any of the design requirements. Everything in contact with the tissue (i.e. molds, force probe, anchors) must be sterilized to prevent contaminations. This can include ethanol, autoclaving, steam, or radiation.

3.2.4 Specifications

The mold has to be a rectangle of dimensions in the range 4 -6 mm in width and 8-10 mm in length. This is to reach confluency within a reasonable amount of time and to have a tissue size that is controllable. The mold has to be made of a polymer with a moderate modulus of elasticity (not too high because we want small strains) and minimal hysteresis to maximize accuracy in strain measurement. Most of the previous research have applied cyclic stresses to the tissue. Strain of 5-15% (1-3 mm) was obtained [42]. Electrical stimulation is usually expressed in terms of electric field, frequency and pulse duration. Based on literature and previous MQPs, the electrical supply should not be above 2.5 V/mm and 3 Hz. Seven days of electrical stimulation should be enough to evaluate the results.

3.3 Design Required Standards

The team should be aware of industry standards when carrying out the project. Failure to follow pre-established international standards can easily result in project failure due to cell death, exposing students and faculty to potential biological hazards, and damage to the environment. A list of standards by the International Standards Organization (ISO) relating to the project is shown below.

Table 2. ISO Standards applying to this project.

ISO 22442-2:2015	Medical devices utilizing animal tissues and their derivatives
ISO 10993-1:2018	Biological evaluation of medical devices
ISO 17422:2018	Plastics -- Environmental aspects -- General guidelines for their inclusion in standards
ISO 7712:1985	Use of disposable micropipettes
ISO 7550:1985	Use of disposable serological pipettes

ISO 22442-2:2015 will be used in this project as it is planned that the initial prototype of the design will be used to culture mouse muscle cells before culturing human muscle cells as a test of the design. ISO 13022:2012 will be used as the end goal of maturing human muscle tissue will require the management of viable human cells. ISO 10993-1:2018 will be used as the device must be biocompatible to house the tissue. ISO 17422:2018 will be used if the final design includes plastic components. ISO 7712:1985 will be used as tissue culture preparation will likely involve the usage of disposable micropipettes. ISO 7550:1985 will likely be used as the project could involve the usage of disposable serological pipettes.

3.4 Revised Client Statement

Based on the identified design requirements and constraints, we revised our client statement to: "Devise a multi-well construct to grow and mature 3D human skeletal muscle tissues for drug testing by mechanically stimulating them to mimic natural environmental conditions."

3.5 Management Approach

In order to work with the time constraint, the team must be efficient in managing the time spent in each process. The project plan is displayed below in Figure 10 using the Gantt chart.

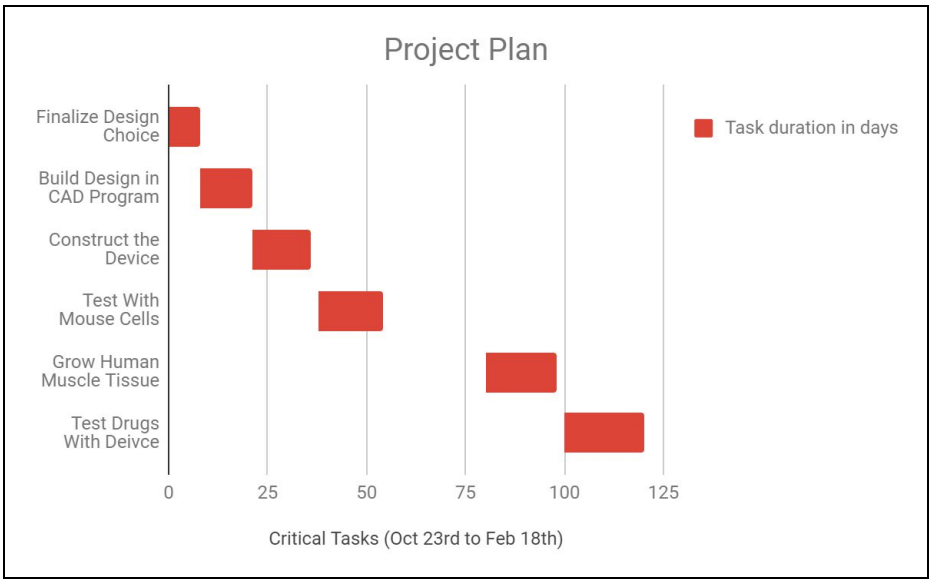

Figure 10. Gantt chart.

The first objective is to finalize the design choice, selecting the overall design concept that will best fulfill the needs of the project. This will take place over the the time period of October 23rd to October 30th. The second step is to finalize the details of the chosen design and construct a model in a Computer Aided Design program. This will take place over the time period of October 30th to November 13th. The third step is to physically construct a working prototype of the device. This will take place over the time period of November 13th to November 27th. The fourth stage is running a preliminary test of the device by using it to mature mouse skeletal muscle tissue. This will take place over the time period of November 29th to December 14th. Following this, the device will be used to grow and mature human skeletal muscle tissue, over a period of time from January 10th to January 28th. These times were decided on as it takes around 16 days for skeletal muscle tissue to mature *in vitro* [42].

Chapter 4: Design Process

The previous chapter identified objectives, constraints, function-means, specifications to understand the design requirements and parameters. This chapter further breaks down the need analysis and evaluate different design alternatives that satisfies the discussed requirements.

4.1 Needs Analysis

The team classified the design requirements into needs and wants based on the client statement and the analyzed constraints. Table 3 below lists the needs on the left column and wants on the right column.

Table 3. Needs and wants list.

Needs	Wants
Mechanically stimulate tissue	Electrically stimulate tissue
Measure contractile force	Measure contractile force, in real time
Support cell proliferation and differentiation	Multi platform construct
Provide anchorage for tissue	Reproducibility for drug screening
Sterilizability	

These functions and means to achieve them are shown in a concept map in Figure 11 below.

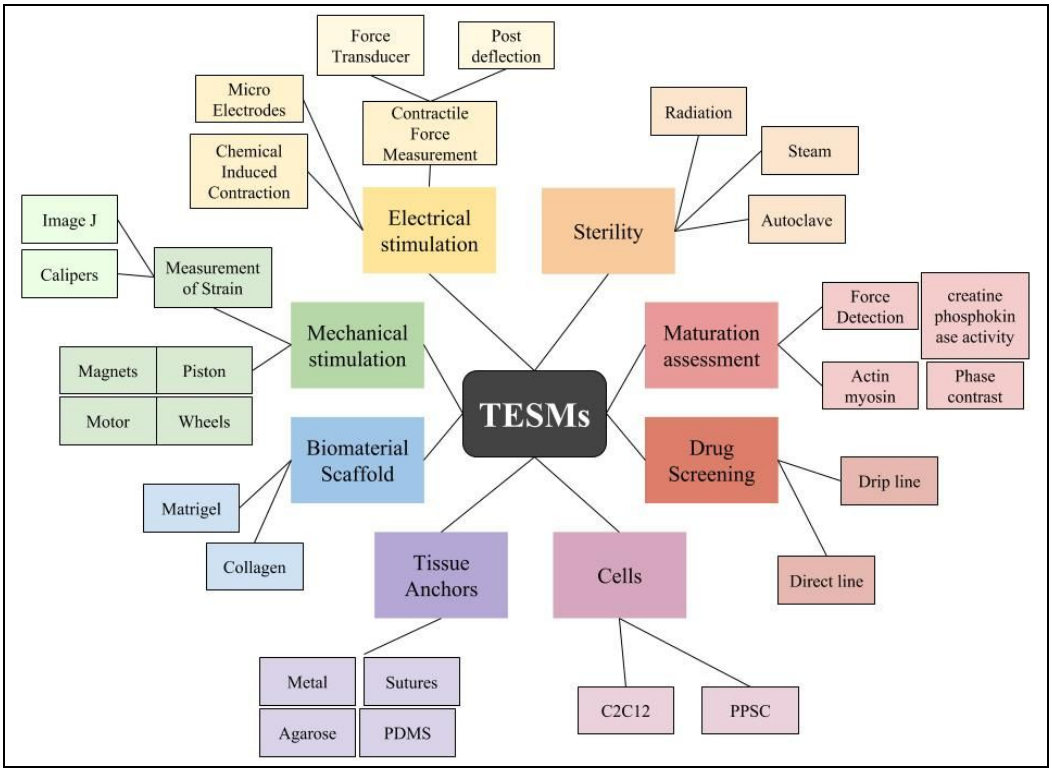

Figure 11. Concept map.

4.2 Alternative Designs

The team adopted Vandenburg's model of PDMS microposts, and this section lists three alternative designs that mechanically deflects the microposts from the bottom of each well.

Alternative Design 1: Pegged/Bumps with wells going down

The first alternative design is a 96 well apparatus that includes a continuous 3D printed base with pegs or bumps that lie directly underneath each well. Bottomless 96 well plates would be brought from a manufacturer and the microposts will be glued on the bottom of each well as shown in Figure 12 below. This piece would go on top of the pegged base, shown below in Figure 13, and move up and down using a screw jack mechanism. The pegged base would push the pdms up and cause the microposts to deflect. Though this alternative design seem feasible, attaching the entire apparatus to the screw jack mechanism is difficult as a small misalignment will cause the microposts to deflect in various angles.

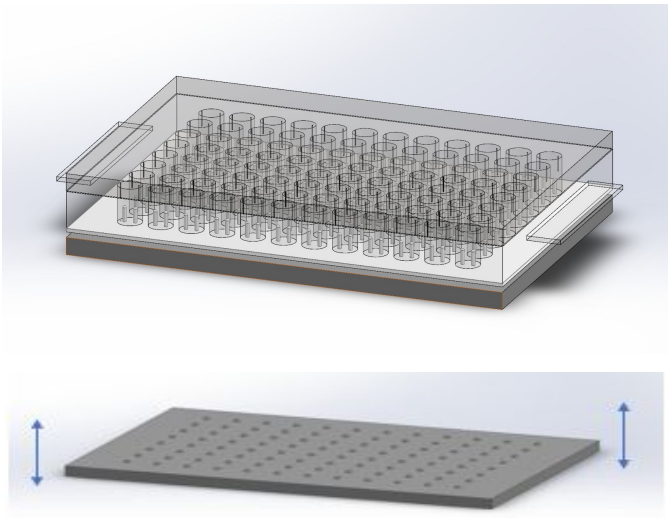

Figure 12. Base with wells and microposts.

Alternative Design 2: Pronged Roller

The pronged roller is located underneath the wells in this alternative design. As the roller rotates, the prongs are brushed against the bottom of the PDMS base, pushing apart the posts to stretch the muscle. There can be a different number of prongs for each well, so the muscle in each well can be stimulated with a different frequency dependent upon the number and spacing of the prongs. However, be the difficulty in maintaining the alignment of the roller so each well would receive the same pressure is a concern. Additionally, the deflection would have been at a moving angle as the prong head dragged across the base, resulting in uneven stimulation. A model of the roller can be seen below in Figure 13.

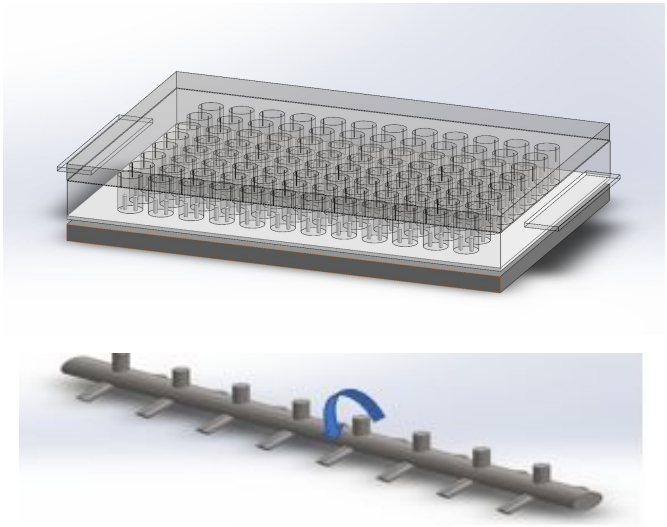

Figure 13. Pronged roller.

Alternative Design 3: Nitinol wires

In this last alternative design, the device is composed of a 6-well plate with two thick PDMS posts at opposite ends of each well. A nitinol wire is tied around each PDMS post and connected to a stainless steel post outside of the well. The aligned stainless steel post will be cyclically heated using a small heating plate on which they will sit. The heat will then be conducted from the stainless steel bar into the nitinol wires which will contract and therefore pull the PDMS posts in the outward direction. The cyclic outward and inward movement of the PDMS posts will cause the tissue to stretch and contract displayed in Figure 14 below. The major limitation of this design is the heating mechanism. The temperature has to be controlled so that no damage is caused to the tissue. Another issue is maintaining a sterile barrier since the wires would perforate the wells. The device also poses a reproducibility issue because the experiment can only be done in 6 wells at a time.

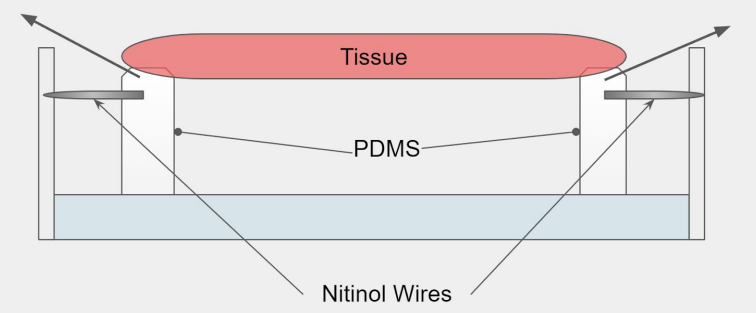

Figure 14. Microposts attached to nitinol wires.

4.3 Experimental methods

Cells can be very difficult to grow, as they require a very specific media and maintenance schedule. This care is taken in order to prevent the cells from dying unexpectedly.

4.3.1 Cell Culture Maintenance

The cell culture procedure are followed using WPI professor Ambady's protocol, which is adapted into many classes. This procedure can be read in full in Appendix D. In simplicity, cells were maintained in media containing many components and growth factors (10% fetal bovine serum (FBS), 2mM glutamax, and 1% penicillin/streptomycin). The cells are subcultured at 50-70% confluency to maintain myogenic potential with 0.05% trypsin/EDTA and phosphate buffered saline (PBS). They are then incubated in more media. Cells differentiation is considered complete when cells fused to form multinucleated myotubes and the nuclei migrate to the peripheral position.

4.3.2 Optimizing Differentiation

A variety of methods have been implemented in prior studies in attempts to induce more ideal degrees of differentiation. Oftentimes, the initial media is designed to inspire growth, and then replaced with media to inspire differentiation. Robert Dennis and Paul Kosnik used a growth media of f12 with 20% FBS for a period of 3-8 days to grow rat myocells before transitioning to a differentiation media of 7% Horse serum for 2-3 weeks [43,44]. Huang et al. grew rat myocells in a 10% FBS 5 ng/ml FGS-2 growth media with a differential media of 6% heat-inactivated FBS [45,46]. Other studies use a third kind of media, maintenance media, to maintain the current status of the cells after growth and differentiation. For example, Vandenburgh grew human muscle cells in a growth media of mgm:skgm 15% FBS for 3 days, moved to a differentiation media of high glucose DMEM 2% Horse serum, where it remained for 5 days, then a mixture of the two prior media for maintenance for 4 weeks [43,47].

4.3.3 Optimizing Tissue Formation

Methods of optimizing tissue formation currently being explored are mainly methods of electrical and mechanical stimulation. The primary methods of mechanical stimulation considered for this project are nitinol molds, molds with magnetic poles, and insertion of prongs to stretch the muscle tissue horizontally and vertically. Methods of electrical stimulation are focused around providing electrical impulses to the tissue during development, to trigger contraction. These two stimuli, mechanical and electrical, mimic the natural conditions of the body, with mechanical stretching replicating the stretching of skeletal muscles during the contraction of opposing muscles, and electrical stimulation replicating electrical signals from neurons in the body, that cause the muscles to contract.

Chapter 5: Design Verification

Three tests were done in order to examine the functionality of the device. The first test conducted was the mechanical stimulation test, which examined the relationship between the air pressure in the air reservoir and the deflection of the PDMS microposts at three different pressures. The second test was the electrical stimulation test, which compared the input voltage through the needles to the electrical field in the media at three different voltages. The last test was the biocompatibility test, which examined the cytotoxicity of the device by seeding C2C12 cells into each well and allowing them to grow without interference for three days.

5.1 Mechanical Stimulation

In order to test if the device would be able to strain the tissue effectively, the percent strain rates were measured at atmospheric pressure and two higher pressures. These pressures were gained using a 5 V battery and a 9 V battery on the air pumps attached to the air reservoirs. Atmospheric pressure in the wells was read at 100.97 kPa. The 5 V battery generated an average pressure of 103.50 kPa, and the 9 V battery generated an average pressure of 116.13 kPa. Pictures of the posts were taken before and after the pressure was applied, and analyzed using ImageJ in order to determine the distance between the posts. An example of these pictures can be seen below in Figure 15.

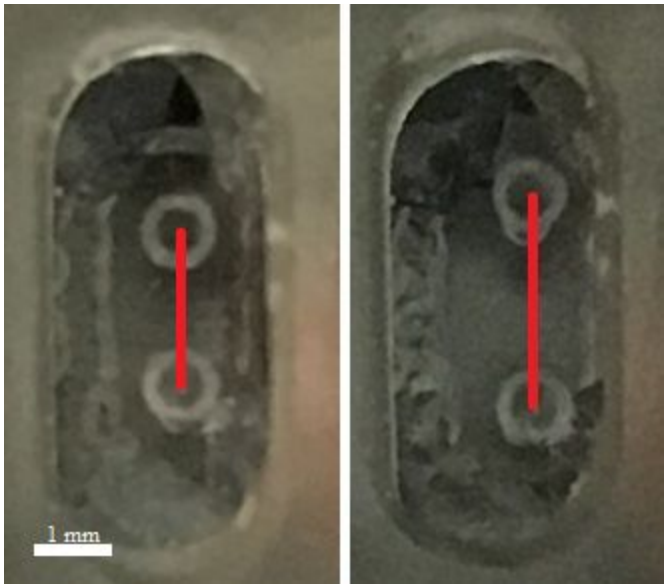

Figure 15. An unpressurized well (left) and a well at 116.13 kPa (right).

The difference in the distance between the posts before and after the pressure was applied was converted into percent strain using Equation 1 below.

$$\frac{Strained\ Distance - Unstrained\ Distance}{Unstrained\ Distance} * 100 = \%\ Strain \qquad (1)$$

The percent strain of the atmospheric pressure was 0, with a standard deviation of zero. This was due to the posts being molded into the exact same shape with a set distance between the posts. Since there was no pressure applied, the distance between the posts did not change. When 103.50 kPa was applied, the percent strain was calculated to be 10.12 ± 0.58. This means that the posts would strain the tissue approximately 10% at 103.50 kPa. When the applied pressure was 116.13 kPa, the percent strain was calculated to be 27.98 ± 1.15. This means that the posts would strain the tissue approximately 30% at 116.13 kPa. A graphical representation of this relationship can be seen below in Figure 16, and Table 4 below summarizes the data discussed.

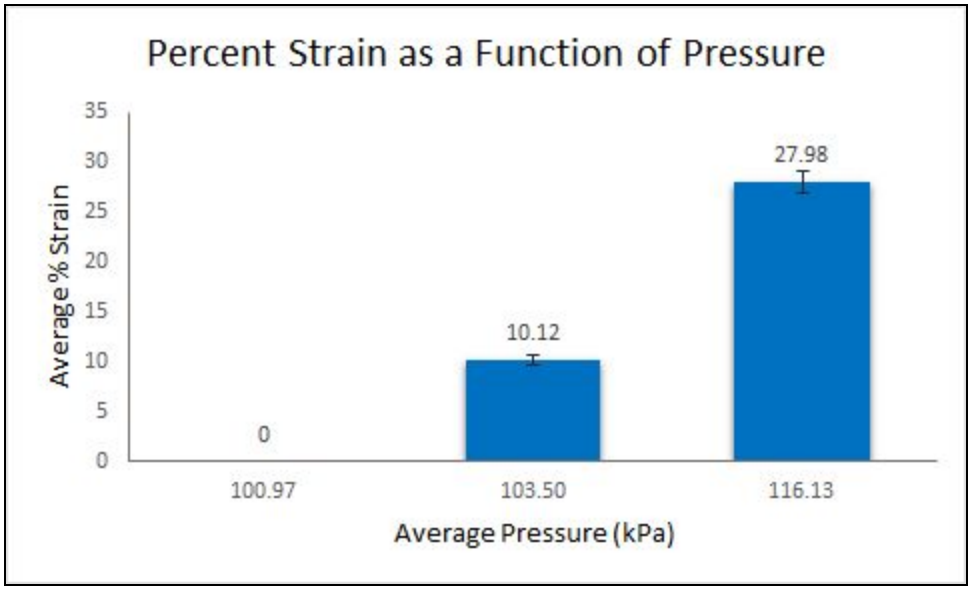

Figure 16. The percent strain as a function of pressure.

Table 4. Mechanical stimulation data

Voltage (V)	Average Pressure (kPa)	Average % Strain	Standard Deviation
0	100.97208	0	0
5	103.503545	10.12	0.5773502692
9	116.13195	27.08	1.154700538

5.2 Electrical Stimulation

A multimeter was used to determine the resistance of a well filled with complete media, and the voltage when a current was passed through the well. The wells were filled with 160 µL of complete media in order to do this test. When testing for the resistance of the media in the well, the measured resistance varied widely between 90 kΩ and 300 kΩ for each well, so no accurate resistance could be determined. For voltage, a voltage on the order of 100 mV was seen, however again the multimeters values fluctuated greatly. In this case, however, the values continued to rise as the multimeter and the electrical leads were held in the complete media. The prolonged electrocution of the complete media lead to hydrolysis of the water and corrosion of the leads in the complete media.

5.3 Biocompatibility

The well plate and lid were sterilized using 70% ethanol. The wells and lid were filled to capacity with the 70% ethanol solution and left to sit for 10 minutes inside a biosafety cabinet. The ethanol was then aspirated and left to evaporate for 20 minutes. Cells were then plated in complete media at 40 thousand cells/well in a total well volume of 150 µL. The cells were incubated (37°C, 5% CO2, 95% humidity) for 3 days in order to assess the cytotoxicity of the device. The cells were counted and subcultured on the 4th day. The cell count result can be seen in Table 5.

Table 5. Cell count per well.

Well #	Total # Cells	Average # Cells	Total Cells in Well
1	35	8.75	8,750
2	104	26	26,000
3	81	20.25	20,250
4	54	13.5	13,500
5	104	26	26,000
6	104	26	26,000
7	110	27.5	27,500
8	85	21.25	21,250
Average # of cells		21,094 cells/well	
Average concentration of cells		210,940 cells/mL	

Chapter 6: Final Design and Validation

The final device is composed of many functional parts, all of which need to meet the safety and industry standards. In addition, there are other considerations that need to be evaluated. These include the economic impact of the device, the ethics of the device, and the manufacturability of the device.

6.1 Design overview

Detailed Models and Drawings (CAD)

The final design of the device can be divided into four major sections. The bottom section, shown in Figure 17 and dimensioned in Figure 18, is referred to as the Base.

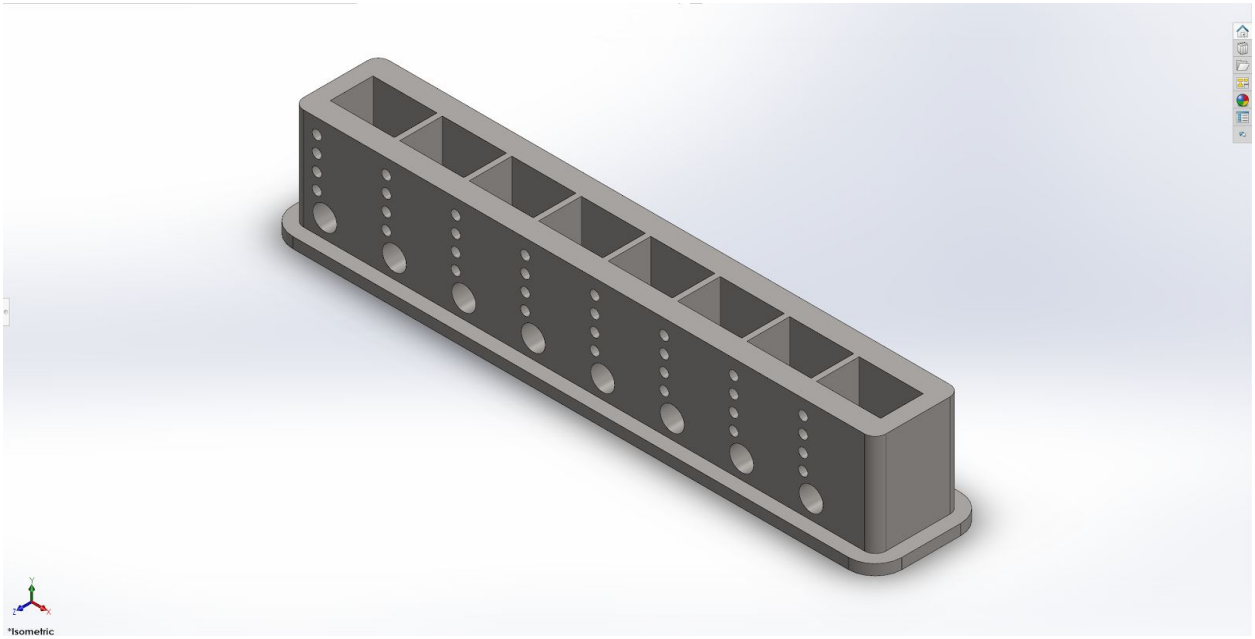

Figure 17. Solidworks model for the base.

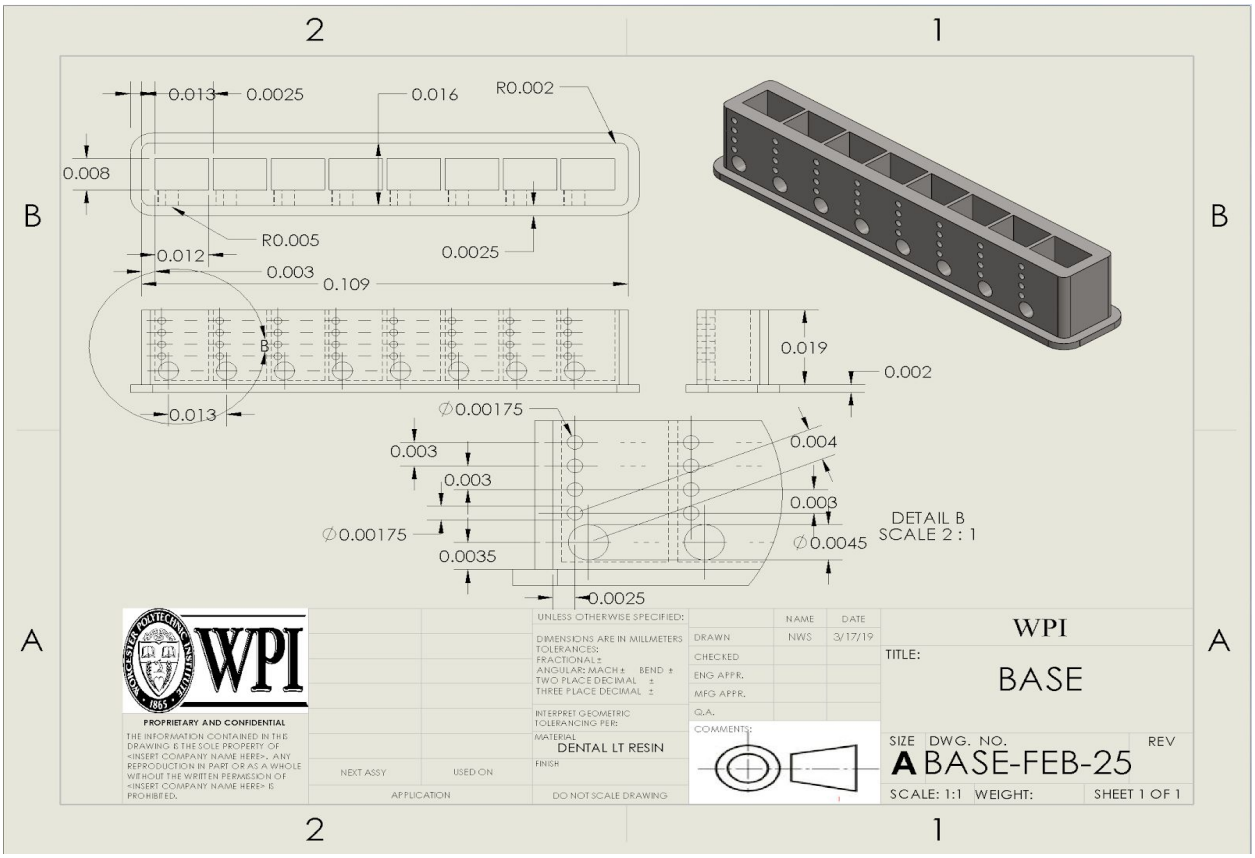

Figure 18. Solidworks drawing for the base.

The Base is constructed of biocompatible Dental LT Resin, and is divided into eight separate chambers. Each chamber is used to contain lightly pressurized air that is used to provide mechanical stimulation to the muscle tissue. Each chamber also contains an air pressure sensor to measure the current air pressure within the chamber. The wide hole at the bottom of the chambers is meant to have an air pump tube put through it. The smaller holes above the air pump hole are for attaching wires to the sensors within – these holes are positioned to be on the left edge of each chamber, to better align with the receivers on the sensors. The base also has a widened bottom for stability. The top of the base is glued with silicone adhesive to the PDMS slab, which will be discussed later.

On top of the PDMS slab is the Well Plate, shown in Figure 19, and dimensioned in Figure 20.

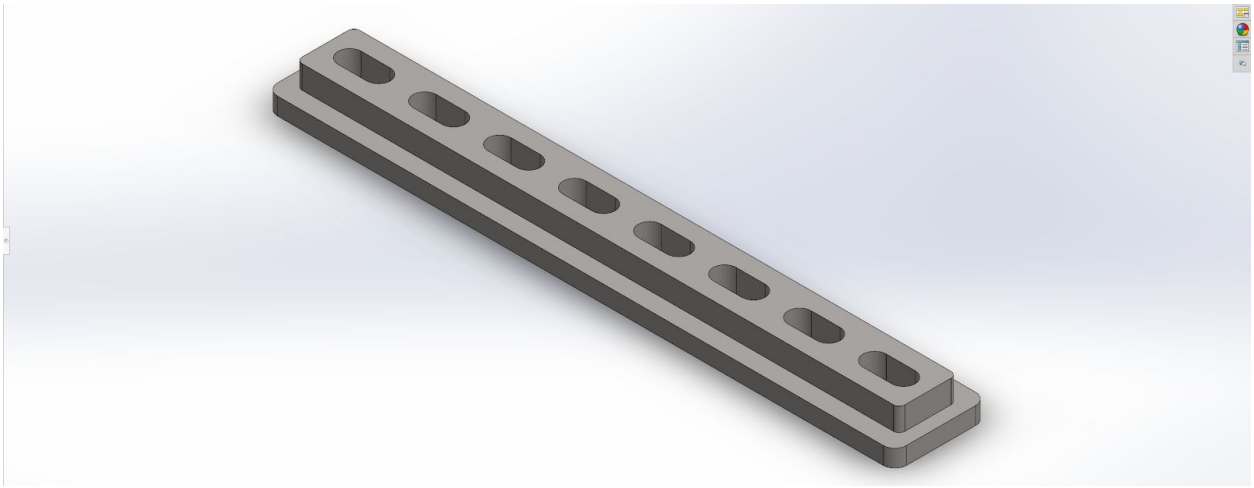

Figure 19. Solidworks model for the well plate.

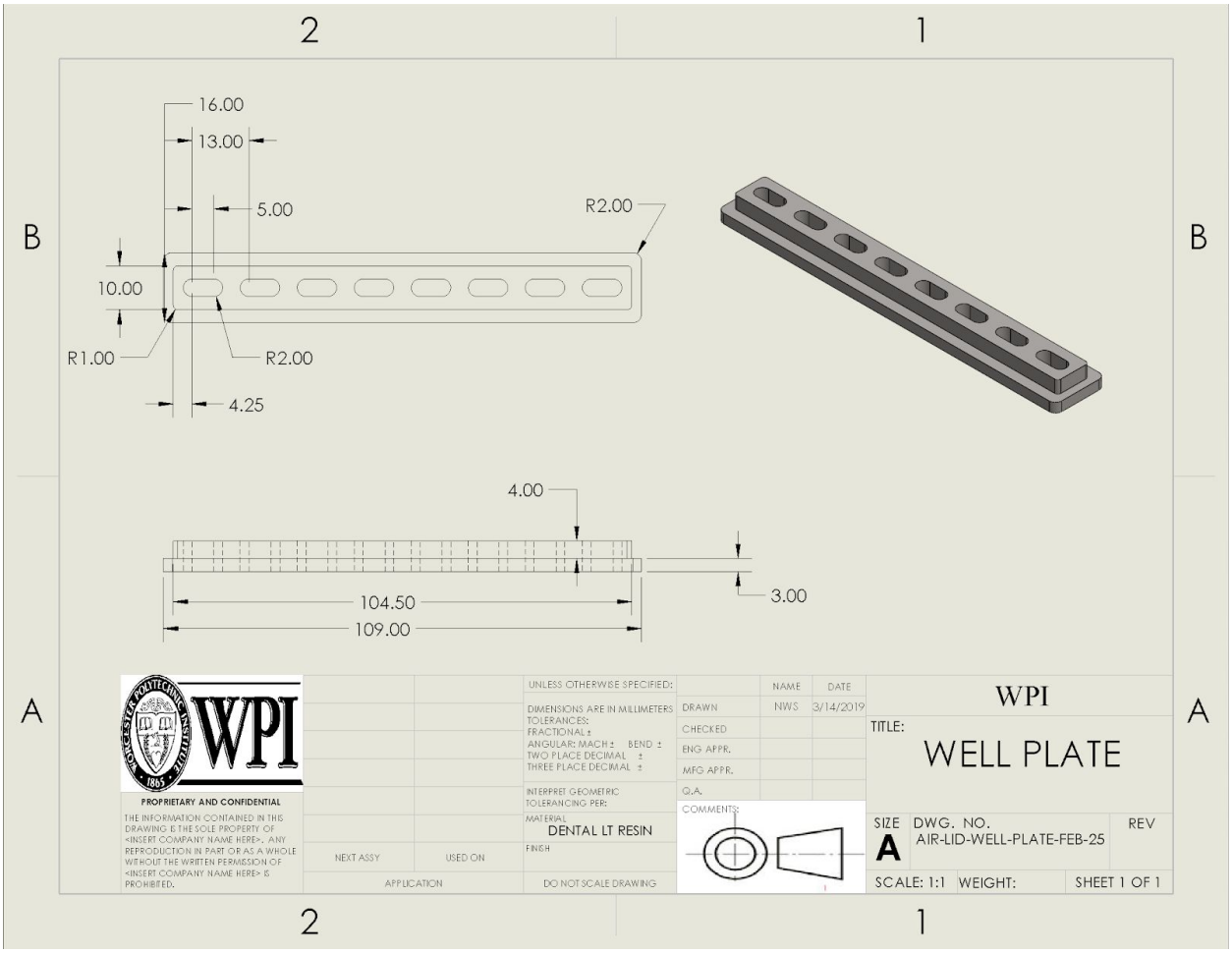

Figure 20. Solidworks drawing for the well plate.

The purpose of the Well Plate, also made of Dental LT Resin is to contain the muscle tissue and accompanying media. The wells are oval-shaped to accommodate for the layout of the of microposts and the direction in which they will deflect when the air pressure in the Base chambers is increased. The PDMS slab is glued to the bottom of the Well Plate with silicone adhesive.

On top of the Well Plate is the Electrode Lid, shown in Figure 21 and dimensioned in Figure 22. The lid is displayed upside down in Figure 21 for 3D printing purposes and visibility of the structures.

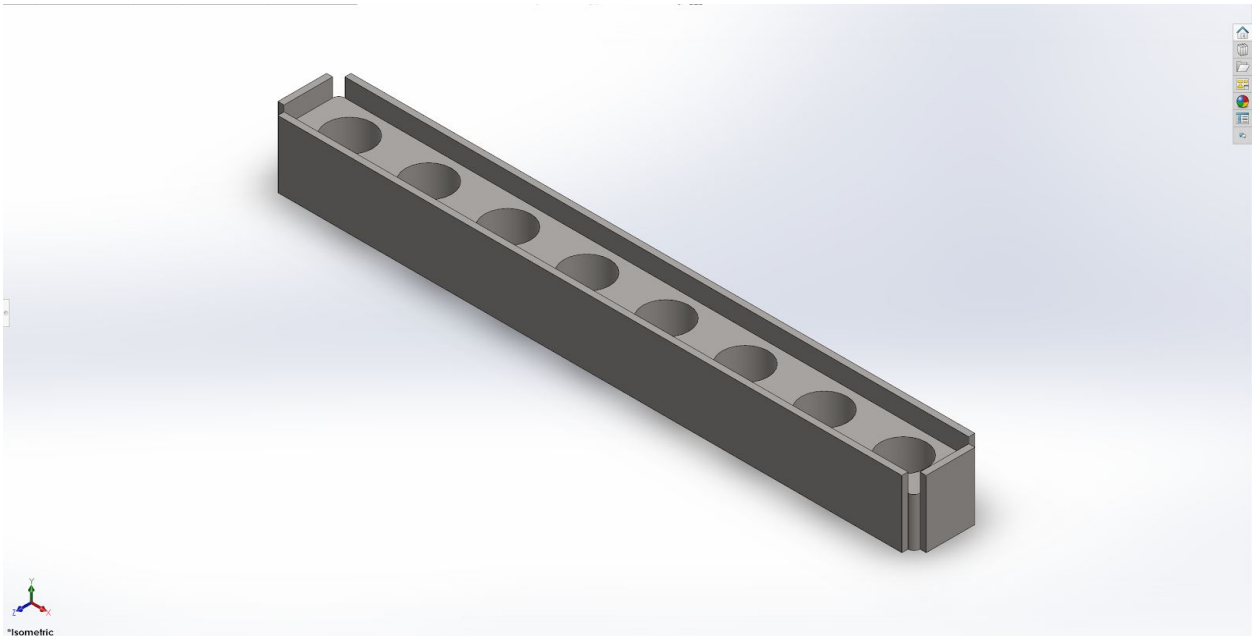

Figure 21. Solidworks model for the electrode lid.

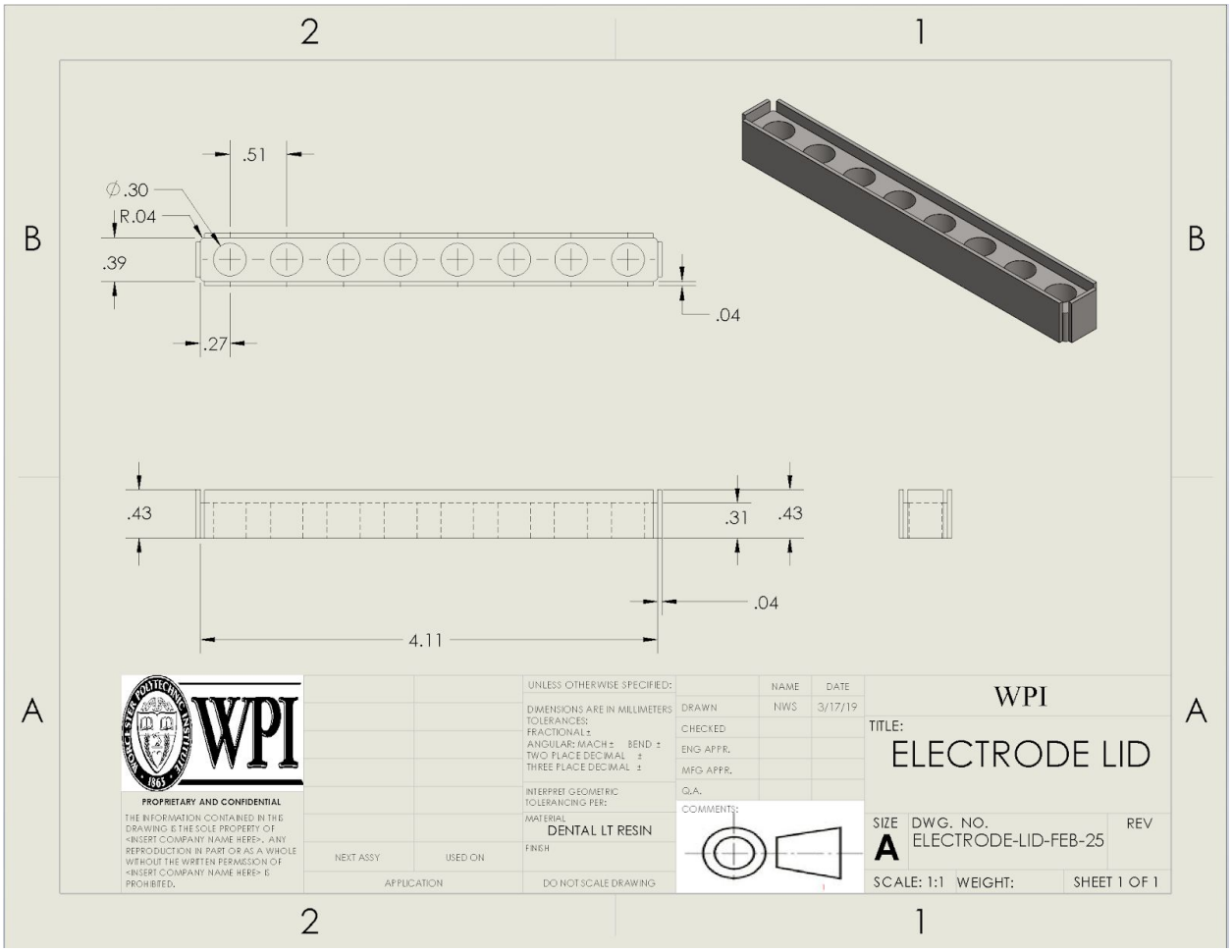

Figure 22. Solidworks drawing for the electrode lid.

The Electrode Lid is also made of Dental LT resin. The electrode lid, designed to keep the culture in the wells from becoming infected while allowing for electrical stimulation, is meant to be placed on top of the Well Plate, with the rectangular protrusions on the sides encasing the top section of the Well Plate, holding the Lid in place. The holes along the length of the Electrode Lid are filled in with rubber stoppers. Through these stoppers are placed two needles each, which reach into the culture media to allow for electrical stimulation.

When in operation, the air pumps will increase the air pressure in the chambers of the Base. The pressure will cause a small bump to appear in the PDMS in the middle of each well. This bubble will cause the microposts to deflect away from each other, mechanically stimulating the muscle tissue. The electrodes will be electrified to electrically stimulate the tissue. The model for the full device is shown in Figure 23.

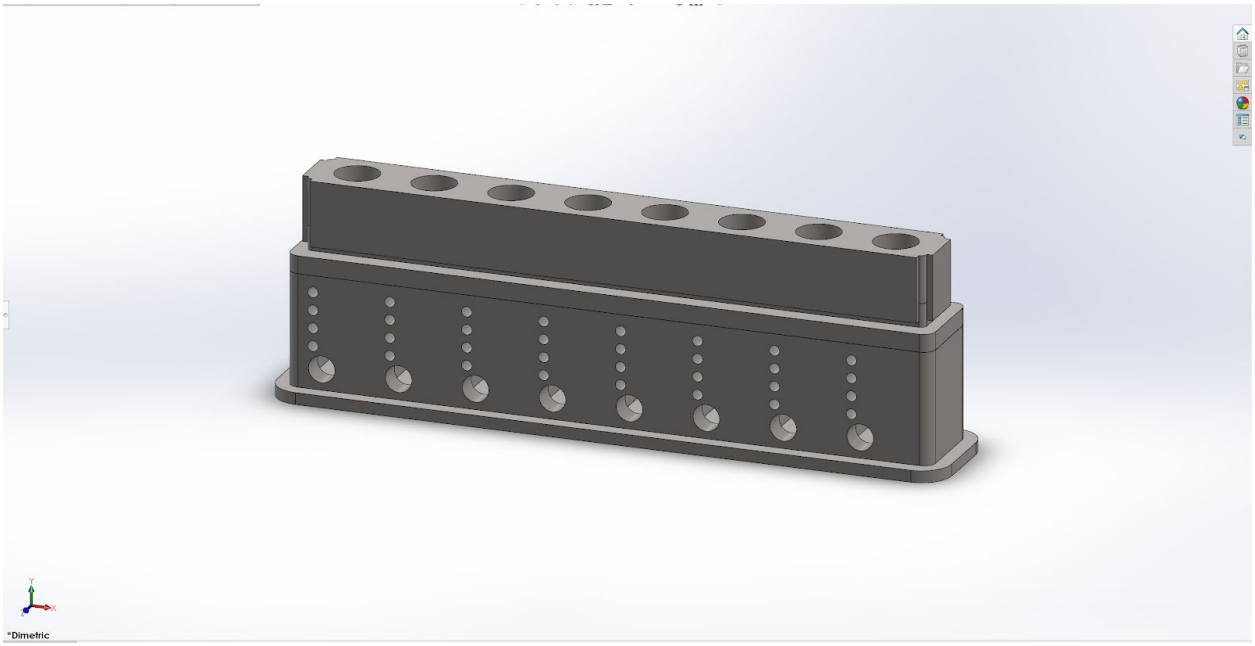

Figure 23. The full device without PDMS, rubber stoppers, or electrical components.

PDMS Micropost and Slab Fabrication

The team adopted Vandenburg's PDMS microposts method to grow tissue in three dimension. The four molds available in Professor Page's lab were used to make individual microposts. A ratio of 1:10 base of silicone elastomer and curing agent was used to fill the molds. The detailed procedure can be found on Myomics Inc. Operating Procedure # DS1.0 or in Appendix C. The set up can be seen below in Figure 24.

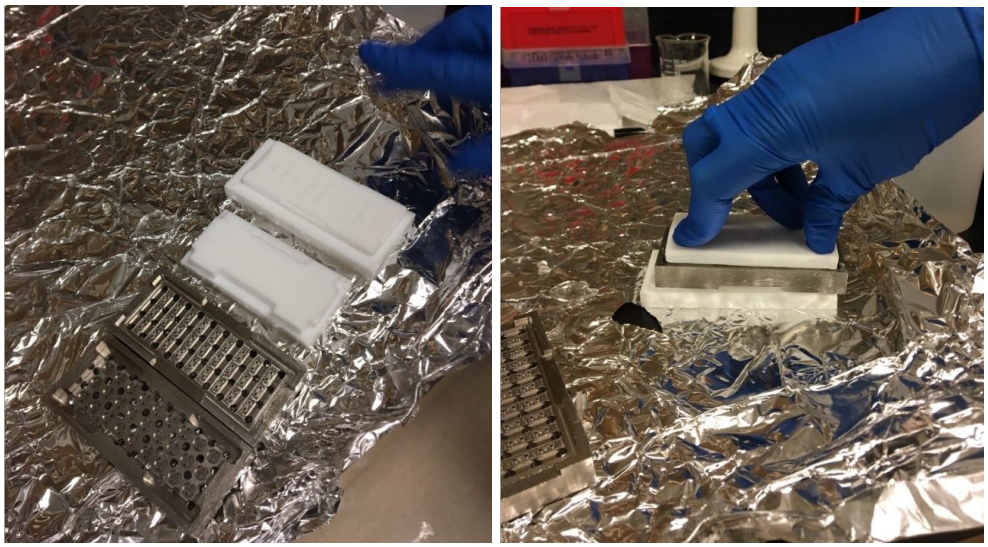

Figure 24. Miroposts mold faces (left) and assembly (right).

The microposts were then cured in Myonics Inc. Binder Oven for 30 minutes at 130℃. After the microposts were cured and extracted from the molds they were stored in a one well plate and the pouring of the bottom PDMS piece was then made. This was done by using 7g of base and 0.7g of curing agent (10:1 ratio) to achieve the right thickness. A sketch of the well rows was made and taped to the base of a Thermo Fisher rectangular cell culture dish. It is important to use the base as the lid can compromise distribution due to concavity. The sketch is also essential to achieve a straight and accurate alignment. 7g of PDMS is poured into the plate and moved around to cover the entire plate. The microposts were carefully placed into the PDMS using forceps and aligned with the well sketch underneath. This was left to cure at room temperature for 48 hours and the set up is demonstrated below in Figure 25. The microposts and base assembly was not cured in an oven, unlike most protocols, in order to ensure minimal changes of the mechanical properties as the microposts would be cured twice.

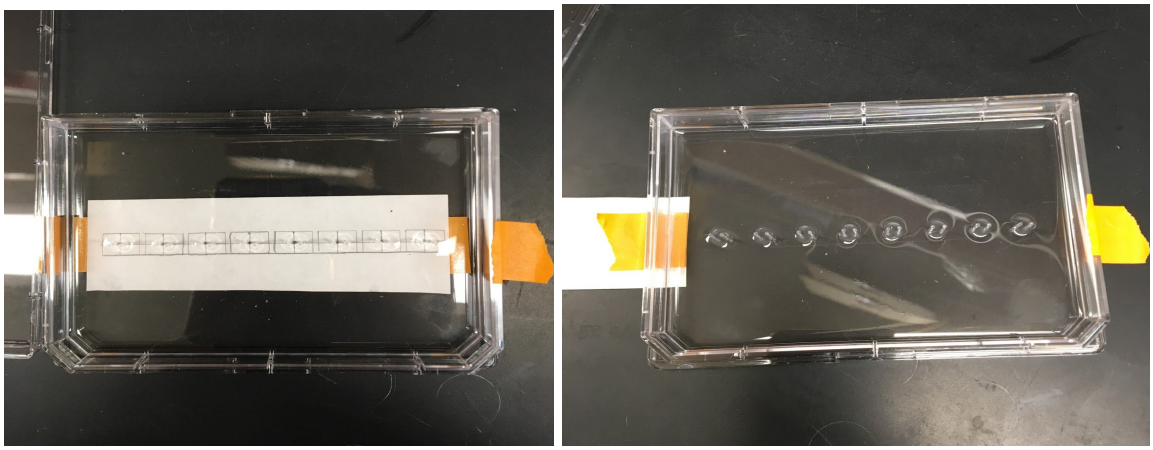

Figure 25. Microposts in PDMS slab with dimension reference (left) and final product (right).

After the PDMS solidified, it was peeled off from the plate and cut to the size of the well apparatus and glued upon using Factor II A-100 Medical Silicone Adhesive.

Electrical Components

The device contained multiple computer components to automate cell growth and record data. Among these items is one Arduino Nano, 8 BMP280 pressure sensors, 8 pressure pumps, and 16 electrodes. The code for these items was programmed in Arduino, a C++ variant. This code controls the device cycle, which consists of the following steps:

1. Pressurizing the chambers to physically stretch the specimens
2. Relaxing the pressurized chambers
3. Activating the electrodes inducing a current through the cells, causing them to contract and decrease the volume of the pressure chamber

4. Record the pressure in the chamber to calculate the pressure induced by the sample, and then calculate the sample strength coefficients.
5. Stop electrode stimulation and proceed from step 1 with individualized strength training for each sample based on their calculated strengths.

This program allows the cells to receive an appropriate strength training regimen, which will avoid tearing weaker samples and enhance growth in stronger samples. The training regimen will consist of 10 minutes of mechanical training, followed by 10 minutes of electrical training, followed by 10 minutes of rest. This cycle will repeat for 3 days, allowing for sufficient time for growth.

Arduino Nano: The Arduino Nano served as the computer used to power different electronic components, and to implement a control system on the device. It operates at 5V and powers the sensors, pressure pumps, and electrodes. It has 2KB of RAM and a 16 MHz clock speed, and does all of the calculations to control the regimen of the muscle samples.

BMP280 Pressure Sensor: HiLetgo High Precision BMP280-3.3 sensors were used for this project. They are 3.3V sensors that are capable of reading temperature and pressure with +/- 1 hPa. We did not use the sensor to record temperature data as the incubators are controlled and it was not relevant to the project. Using the pressure recorded from the sensors, approximate sample strength could be calculated. These sensors were fitted inside the pressure chambers.

Pressure Pump: The pressure pumps used are 3V DC pumps that can produce approximately 20-30 kpa of pressure. Due to the small size of the pressure chambers and the small differences in pressure required, a large pump could have been too forceful, and would have consumed more power and made the device larger. By powering the pumps with a specific voltage the pressure induced can be controlled. One alternative 12V DC pump was used for testing.

Electrodes: 27 (½) gauge 316 stainless steel hypodermic needles were used to pass voltage through the tissue for electrical stimulation. Two needles were inserted through each rubber stopper, and copper wire was wrapped around each needle and connected to the Arduino. The lid with needles and wire setup are displayed in Figure 26 below.

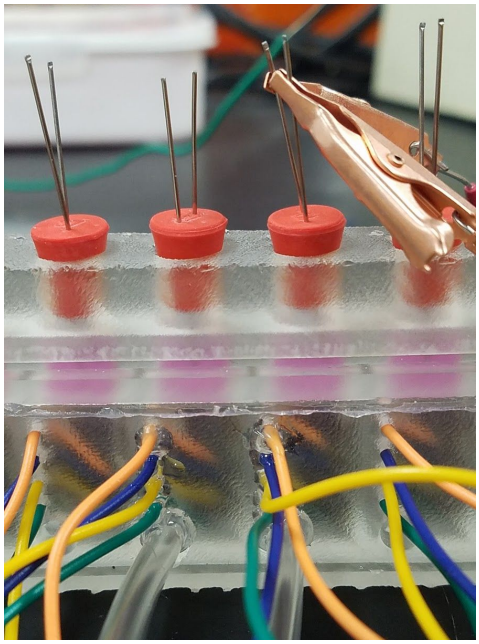

Figure 26. The device with needles and one example wired well.

The entire design setup with all the components can be seen below in Figure 27.

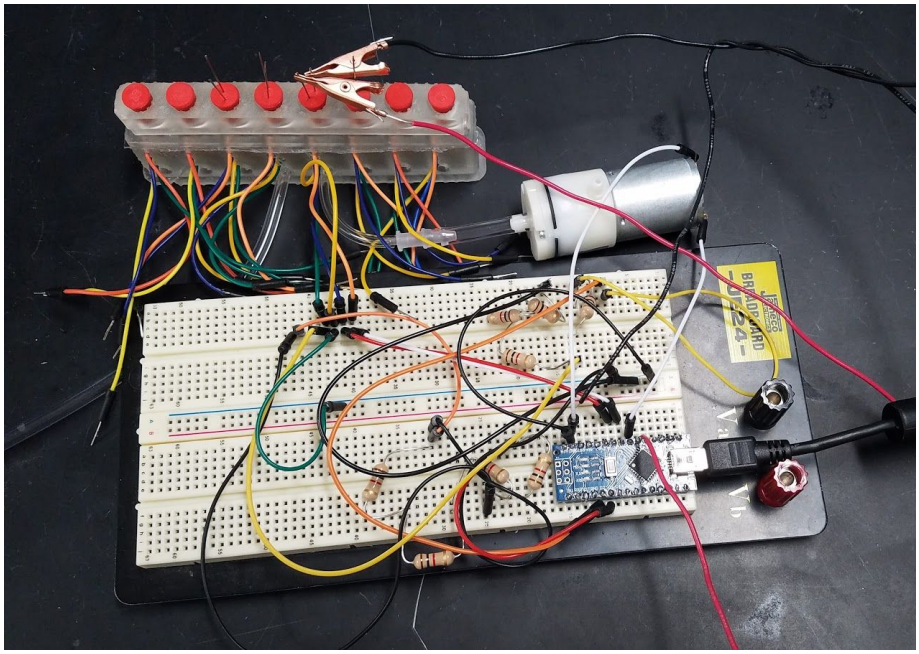

Figure 27. Final design setup.

6.2 Industry Standards

The team was aware of industry standards when carrying out the project. Failure to follow pre-established international standards could have easily resulted in project failure due to cell death, exposed students and faculty to potential biological hazards, and caused damage to the environment. Table 2 in Section 3.3 listed the necessary ISO Standards that this project must follow, copied below in Table 6.

Table 6. ISO Standards applying to this project.

ISO 22442-2:2015	Medical devices utilizing animal tissues and their derivatives
ISO 13022:2012	Management of viable human cells
ISO 10993-1:2018	Biological evaluation of medical devices
ISO 17422:2018	Plastics -- Environmental aspects -- General guidelines for their inclusion in standards
ISO 7712:1985	Use of disposable micropipettes
ISO 7550:1985	Use of disposable serological pipettes

ISO 22442-2:2015 will be used in this project as it is planned that the initial prototype of the design will be used to culture mouse muscle cells before culturing human muscle cells as a test of the design. ISO 13022:2012 will be used as the end goal of maturing human muscle tissue will require the management of viable human cells. ISO 10993-1:2018 will be used as the device must be biocompatible to house the tissue. ISO 17422:2018 applies to this project as the 3D printed components of the project are made of plastic. ISO 7712:1985 and ISO 7550:1985 both apply to this project as disposable micropipettes and disposable serological pipettes are have been and are used to manage cell cultures.

6.3 Economic Impact

The device's most prominent economic impact lies in the reduction of the drug development cost. As mentioned in Chapter 2, the development of drugs for muscular diseases is very costly (money, time, resources) and still inefficient as most drugs fail in phase II of clinical trials. The device would allow a considerable reduction in money spent in order to test the efficiency of drugs on laboratory-grown tissue before releasing them for clinical trials. This would also result in a reduction of time spent on developing inefficient drugs as the efficiency will be determined early on in the development process. The device is entirely made of affordable materials and can

be assembled and operated within a timespan of a few weeks, maximizing the economic benefits for the user. An indirect impact would also be a reduction of drug costs. Since the drug development process would be less costly, the prices of the drugs will also decrease. Therefore, our device does not provide economic benefits to the users only but to patients as well.

6.4 Ethical Concerns

The major ethical concern of the health-related issues is mostly drug testing. To this day, the debate on whether it is ethical to test for drugs on animals is still very present within the scientific community. Conventional studies would test on animals then test on humans. However, even though participants to clinical trials are asked for consent before they enter the trial, there are still ethical concerns around the issue. This is due to the risk of negative side effects that may result, including impairment and fatality. This device could help reduce this problem by testing *in vitro* human tissue rather than on live subjects. It is required that drugs need to be tested on humans at some point before commercialization, but the casualties could be reduced through the use of prior *in vitro* screenings.

6.5 Manufacturability

The device can be easily manufactured and is relatively inexpensive. In conformity with initial objectives, the design offers the possibility of conducting reproducible experiments. The individual components of the design are easy to manufacture at a reasonable cost and within a moderate time frame.

Chapter 7: Discussion

This project was designed in order to achieve differentiating and exercising skeletal cells, specifically C2C12 myocytes, into adult skeletal tissue. The device needed to stimulate the cells both mechanically and electrically, applying strain to stretch the tissue and voltage to cause it to contract. Additionally, the contractile force of the tissues needed to be measurable, so their maturation and strength could be observed. The device also needed to be multi-welled, so that a high throughput could be achieved. Through the design of the device and three tests, the device was shown to be capable of meeting those objectives.

7.1 Mechanical Stimulation

As stated in the literature review, most studies have used between 10% and 60% strain for stretching muscle tissue for mechanical stimulation, with the most positive results occurring with strains between 20% and 30%. Therefore, the results of the post deflection testing are very encouraging. The average percent strain at 9V of power supplied to the device was 27.98%, within the ideal range of 20% to 30%. This number would, however, be impacted if cells were seeded and muscle tissue developed between the microposts, as the tissue would provide a very small amount of resistance to the stretching. This resistance would likely be negligible, as 3D lab-grown muscle tissue has historically only managed to output forces in the milliNewtons, and only when fully grown to the extent that the device can grow them to. If different values of strain were required, they could be reached by supplying different voltages. The amount of strain is limited, however, as the PDMS can only stretch so much before it either ruptures or cannot stretch any further. However, this should not be a significant limitation, as muscle tissue does not need to have significantly more strain put on it than we've shown the device can deliver.

Because this test showed that the pressure in the air reservoir and the curvature of the basement PDMS is related, it also showed that measuring the contractile force the tissue is capable of is possible. As the tissue contracted, it would deform the basement PDMS, changing the air pressure in the air reservoir. A limitation of this would be if the contractile force is too small to significantly affect the basement PDMS, but this is a negligible concern. Tissue that would be incapable of the force necessary to deform the basement PDMS would be unorganized and would not serve as a proper model of adult skeletal tissue.

7.2 Electrical Stimulation

The electrical stimulation tests proved problematic to gather data from. Due to the inconsistencies when measuring voltage and resistance, no usable information could be gathered.

The multimeter was tested using known resistors, which produced accurate non-varying results, and on 9V batteries for voltage, which also produced accurate non-varying results. The problems with measuring voltage and resistance appear to stem from the fact that the complete media is a liquid. However, we did see a reaction in the media due to the current passing through, namely the formation of bubbles. These bubbles proved that the needles were in fact delivering a consistent current to the media, though likely at a too high voltage.

7.3 Cytotoxicity

The cell count, performed three days after the cells were initially introduced to the device, counted an average of 21,094 cells/well. This is roughly half of the number of cells introduced to each well. While ideally there would have been the same number of cells as the beginning, or more than were initially seeded, this is still considered a successful cytotoxicity test by the group, as more than half of the cells survived, indicating that the device does not provide an actively hostile environment to the cells. Additionally, the decrease in cell count could be attributed to the fact that the cells consumed all nutrients available in the media before the three day mark, or that that each well may only have the space to adequately support about 20,000 cells. The low cell count could also be caused by low cell adhesion to the PDMS, as it was not tested for hydrophobicity. This test had limitations in that the wells were not imaged as soon as they could be, due to the fact the team could not locate a non-inverted microscope for some time to image the wells with. However, the cells were extracted and counted to supplement for this.

Chapter 8: Conclusions and Recommendations

The final device, as constructed, is biocompatible and capable of mechanically and electrically stimulating muscle tissue to promote successful maturation into healthy adult skeletal muscle tissue. Additionally, the device was inexpensive to produce the initial prototype of, implying producing further models would be even cheaper. However, further work is required to fully develop the device into a working model. If this device were built into a functional product, it would doubtlessly be an invaluable contribution to the medical field as a step in clinical studies for drug testing and disease modeling.

Even with the device in its current state, for future MQPs that have methods, objectives, or resources in common with this one, this MQP can provide helpful recommendations.

When using cell lines, it is incredibly helpful to have at least two plates going for the cells, especially with muscle cells. Should one plate become overly confluent and stop proliferating, or become contaminated, the other plate will still have viable cells to use. This is useful if parts of the MQP take longer than expected, and the cells are not able to be used as soon as anticipated. Note this is only beneficial if care is taken to prevent cross contamination during cell passaging, or double the normal amount of resources will be used with no added security. With muscle cells, be stringent with subculturing, or the plate will become overly confluent and stop proliferating. Once future devices are tested with non-human cultures, such as C2C12 cells, test again with human muscle tissue. When using human cell lines, be extremely cautious to avoid the possible spread of bloodborne pathogens. Additionally, care should be take to not plate too many cells or allow them to go too long without replacing the media, as they may not have the necessary space or resources to continue dividing at a certain point, especially if the wells are small as in this project.

For 3D printing, make sure all dimensional values and requirements are known before placing orders. Be sure to include for tolerances and error when designing the parts in computers aided design software. Print with the simplest, easiest materials that can be used, if not all parts of the device have the same requirements. Consider employing multiple sources for 3D printed components, including those outside of WPI, to decrease the negative impacts of long delays and warped pieces.

The most difficult part of the assembly was ensuring the PDMS microposts lined up perfectly to the bottom of the wells after curing. After trying different molds, the best result was from using the bottom of a rectangular one well plate. Minimal movements was essential and the microposts were fixed again after taping down the well. However, PDMS is very viscous and the microposts

were still not perfectly aligned in the center of each well. This is a problem as deflections can vary based on where the microposts are located. A method of securing down the microposts in the exact location would save a lot of time. In addition, it took many trials to get the right thickness of the slab because too thin would cause the PDMS to rip and too thick means it would take greater pressure to deflect the posts. If given more time, the team would create a whole mold for this component.

The electrical and digital components of the project posed an additional challenge to a team of mostly biomaterial focused biomedical engineers. The primary difficulty encountered with the electrical components of the device was inconsistent performance. While the final voltage produced by the Arduino was always just under 5V, the actual voltage the sensors received under the same wiring conditions varied from expected values, and the addition of multiple sensors continued to affect the voltage in unexpected ways. Multiple outside sources with wiring experience were consulted and the actual problem was hard to pinpoint. Due to the cheapness of the components it would be a feasible alternative to simply buy additional arduinos to set up multiple systems.

The arduino development environment is very bare bones, but given one team member had previous programming experience it did not prove too difficult. Using documentation of the sensor, and available libraries for the sensor, the code for the project was fairly straightforward. However, due to the nature of low level computers such as the arduino, some difficulties were encountered with commands not being fully completed. Essentially, the arduino would read command 1, start to complete it, and then go to command 2, and cut off command 1. This was fixed using short delays to ensure the program had sufficient time to complete longer commands. It is important that any team working on a similar project have at least one person with computer science experience to write code efficiently.

Electrical stimulation posed unexpected issues with the team. Firstly, excessive voltage in the complete media resulted in hydrolysis of the liquid, which was unexpected. Additionally, the leads appeared to corrode/accumulate interfering materials, which may have contributed to the inconsistent results. Measuring resistance was equally problematic, values were similarly highly varied. The team was able to easily measure values of batteries, the arduino, and resistors, so the difficult component appears to be the complete media. The problematic behavior of the complete media prevented accurate data from being recorded. Our recommendations are to use non-corrosive needles with the media and to use a multimeter specifically meant for use with liquids.

While straightforward, an additional difficulty of this project was soldering the sensors together. The sensors needed to rest in small wells, and each needed to be soldered in 6 places, closely

together. During soldering, the solder for two pins would frequently become intertwined, forcing them both to be redone. Furthermore, these connections also frequently came loose when forcing the sensor into the pressure chamber. Fortunately once the sensor was in the pressure chamber and confirmed to be functioning none of them caused further problems. This issue could have been avoided by making the air reservoir chambers slightly bigger, so less force was needed to place the sensors inside, as well as using a more precise soldering gun with a very narrow tip.

For future similar projects, there are several points of frustration that could easily be avoided. Firstly, using SPI rather than I2C would make routing multiple sensors to one arduino simpler, as there were only 2 distinct addresses for I2C, this required a unique configuration to use multiple sensors. Furthermore, rather than focusing on getting one component working for all the wells, it would be more fruitful to complete every feature for one well, and then expand it one well at a time until all wells were functional. This would also help to determine future problems earlier, and less wasted time if a given solution was actually problematic. Finally, enlisting either a student or professor in the ECE department would help with troubleshooting the wiring and electrical issues, as no one on the team had significant experience with electrical engineering.

It is important to think about all steps of the projects and be careful about all the constraints such as imaging instruments. The team overlooked this minor detail which became a huge problem later on. The team was not able to image the cells for the biocompatibility test because the only available microscopes were inverted and the electrical components bulky and in the way of the scope. In the future, it would be necessary to fix the well in a non-permanent way. That way, the well plate can be separated from the apparatus for imaging.

References

[1] T. Vos *et al.*, “Global, regional, and national incidence, prevalence, and years lived with disability for 328 diseases and injuries for 195 countries, 1990–2016: a systematic analysis for the Global Burden of Disease Study 2016,” *The Lancet*, vol. 390, no. 10100, pp. 1211–1259, Sep. 2017.

[2]. “Myotonic dystrophy type 1 | Genetic and Rare Diseases Information Center (GARD) – an NCATS Program.” [Online]. Available: https://rarediseases.info.nih.gov/diseases/8310/myotonic-dystrophy-type-1.

[3] “How many people are affected by or are at risk of muscular dystrophy?,” *http://www.nichd.nih.gov/*. [Online]. Available: http://www.nichd.nih.gov/health/topics/musculardys/conditioninfo/risk.

[4] “Duchenne Muscular Dystrophy (DMD),” *Muscular Dystrophy Association*, 17-Nov-2017. [Online]. Available: https://www.mda.org/disease/duchenne-muscular-dystrophy.

[5] J. D. Walston, “Sarcopenia in older adults,” *Curr Opin Rheumatol*, vol. 24, no. 6, pp. 623–627, Nov. 2012.

[6] P. Burlina, S. Billings, N. Joshi, and J. Albayda, “Automated diagnosis of myositis from muscle ultrasound: Exploring the use of machine learning and deep learning methods,” *PLOS ONE*, vol. 12, no. 8, p. e0184059, Aug. 2017.

[7] M. Middlesworth, “The Cost of Musculoskeletal Disorders (MSDs) [Infographic],” *ErgoPlus*, 23-Jul-2015.

[8] DonSeiffert, “Report suggests drug-approval rate now just 1-in-10,” *Amplion*, [Online]. Available: https://www.amplion.com/inthenews/report-suggests-drug-approval-rate-now-just-1-in-10.

[9] S. Caddeo, M. Boffito, and S. Sartori, “Tissue Engineering Approaches in the Design of Healthy and Pathological I*n Vitro* Tissue Models,” *Front Bioeng Biotechnol*, vol. 5, Jul. 2017.

[10] “Myotonic dystrophy type 1 | Genetic and Rare Diseases Information Center (GARD) – an NCATS Program.” [Online]. Available: https://rarediseases.info.nih.gov/diseases/8310/myotonic-dystrophy-type-1.

[11] P. Burlina, S. Billings, N. Joshi, and J. Albayda, “Automated diagnosis of myositis from muscle ultrasound: Exploring the use of machine learning and deep learning methods,” PLOS ONE, vol. 12, no. 8, p. e0184059, Aug. 2017.

[12] “Duchenne muscular dystrophy | Genetic and Rare Diseases Information Center (GARD) – an NCATS Program.” [Online]. Available: https://rarediseases.info.nih.gov/diseases/6291/duchenne-muscular-dystrophy.

[13] “Duchenne Muscular Dystrophy (DMD),” Muscular Dystrophy Association, 17-Nov-2017. [Online]. Available: https://www.mda.org/disease/duchenne-muscular-dystrophy.

[14] J. D. Walston, “Sarcopenia in older adults,” Curr Opin Rheumatol, vol. 24, no. 6, pp. 623–627, Nov. 2012.

[15] “The Drug Development and Approval Process: FDAReview.org.” [Online]. Available: http://www.fdareview.org/03_drug_development.php.

[16] S. Loretta, “Muscular System.” [Online]. Available: http://www.drstandley.com/bodysystems_muscular.shtml.

[17] BC Campus “10.2 Skeletal Muscle – Anatomy and Physiology.” [Online]. Available: https://opentextbc.ca/anatomyandphysiology/chapter/10-2-skeletal-muscle/.

[18] Gillies, A. R., & Lieber, R. L. (2011). Structure and Function of the Skeletal Muscle Extracellular Matrix. *Muscle & Nerve*, 44(3), 318–331. http://doi.org/10.1002/mus.22094

[19] Kentucky Community and Technical College System, “Muscular System: Stages of A Muscle Contraction.” [Online]. Available: http://legacy.owensboro.kctcs.edu/gcaplan/anat/Notes/API%20Notes%20J%20%20Muscle%20Contraction.htm.

[20] BC Campus, “12.4 The Action Potential - Anatomy and Physiology.” [Online]. Available: https://opentextbc.ca/anatomyandphysiology/chapter/12-4-the-action-potential/.

[21] McGraw-Hill Animations. “Muscle Contraction Process [HD Animation].” [Online]. Available: https://www.youtube.com/watch?v=ousflrOzQHc.

[22] P. M. Hopkins, “Skeletal muscle physiology,” *Continuing Education in Anaesthesia Critial Care & Pain,* 6(1), 1-6. Available: https://academic.oup.com/bjaed/article/6/1/1/347004

[23] Charrasse, S., Causeret, M., Comunale, F., Bonet-Kerrache, A., & Gauthier-Rouvière, C. (2003), “Rho GTPases and cadherin-based cell adhesion in skeletal muscle development,” *Journal of Muscle Research & Cell Motility*, 24(4-6), 311-315.

[24] I. Pasteur, "Muscle Regeneration", *YouTube*, 2017. [Online]. Available: https://www.youtube.com/watch?v=VBKC0mItPZs. [Accessed: 19- Sep- 2018].

[25] Maganaris, C. N., “Force–length characteristics of in vivo human skeletal muscle.” *Acta Physiologica Scandinavica*, *172*(4), 279-285. Available: https://www.ncbi.nlm.nih.gov/pubmed/11531649/

[26] Edwards, R. H. T., Young, A., Hosking, G. P., & Jones, D. A., “Human skeletal muscle function; description of tests and normal values,” *Clinical Science and Molecular Medicine,* 52, 283-293. doi: 10.1042/cs0520283.

[27] CDC, “Body Measurements.” [Online]. Available: https://www.cdc.gov/nchs/fastats/body-measurements.htm.

[28] Pan, N. “LENGTH OF LONG BONES AND THEIR PROPORTION TO BODY HEIGHT IN HINDUS,” *Europe PMC,* [Online]. Available: https://europepmc.org/backend/ptpmcrender.fcgi?accid=PMC1249729&blobtype=pdf.

[29] Racca, A. W., et al, “Contractility and kinetics of human fetal and human adult skeletal muscle,” *The Journal of Physiology*, 591(12), 3049-3061. Available: https://www.ncbi.nlm.nih.gov/pmc/articles/PMC3832119/.

[30] “Current Price List | Laboratory Animal Services,” *The University of Adelaide*. [Online]. Available: https://www.adelaide.edu.au/animal-services/products/price/.

[31] S. Chen, T. Nakamoto, N. Kawazoe, and G. Chen, “Engineering multi-layered skeletal muscle tissue by using 3D microgrooved collagen scaffolds,” *Biomaterials*, vol. 73, pp. 23–31, Dec. 2015.

[32] A. Fatehullah, S. H. Tan, and N. Barker, "Organoids as an *in vitro* model of human development and disease," *Nature Cell Biology*, 01-Mar-2016. [Online]. Available: http://link.galegroup.com.ezproxy.wpi.edu/apps/doc/A446521917/AONE?sid=googlescholar. [Accessed: 24-Sep-2018].

[33] Y. Ikada, "Challenges in tissue engineering," *J R Soc Interface*, vol. 3, no. 10, pp. 589–601, Oct. 2006.]

[34] S. Rangarajan, L. Madden, and N. Bursac, "Use of Flow, Electrical, and Mechanical Stimulation to Promote Engineering of Striated Muscles," *Ann Biomed Eng*, vol. 42, no. 7, pp. 1391–1405, Jul. 2014.

[35] R. B. Sadeghian, M. Ebrahimi, and S. Salehi, "Electrical stimulation of microengineered skeletal muscle tissue: Effect of stimulus parameters on myotube contractility and maturation," *Journal of Tissue Engineering and Regenerative Medicine*, vol. 12, no. 4, pp. 912–922, Apr. 2018.].

[36] S. Breslin and L. O'Driscoll, "Three-dimensional cell culture: the missing link in drug discovery," *Drug Discovery Today*, vol. 18, no. 5, pp. 240–249, Mar. 2013.

[37] "Tissue Engineering: Current Strategies and Future Directions." [Online]. Available: https://www-ncbi-nlm-nih-gov.ezproxy.wpi.edu/pmc/articles/PMC3214857/. [Accessed: 24-Sep-2018].].

[38] Somers, S. M., Spector, A. A., DiGirolamo, D. J., & Grayson, W. L., "Biophysical Stimulation for Engineering Functional Skeletal Muscle," *Tissue Engineering. Part B, Reviews*, 23(4), 362–372. doi: 10.1089/ten.teb.2016.0444.

[39] Powell, C. A., Smiley, B. L., Mills, J., & Vandenburgh, H. H., "Mechanical stimulation improves tissue-engineered human skeletal muscle," *American Journal of Physiology,* [Online]. Available: https://www.physiology.org/doi/full/10.1152/ajpcell.00595.2001.

[40] H. H. Vandenburgh, S. Hatfaludy, P. Karlisch, and J. Shansky, "Mechanically induced alterations in cultured skeletal muscle growth," *Journal of Biomechanics*, vol. 24, pp. 91–99, Jan. 1991.

[41] Park, H., et al., "Effects of electrical stimulation in C2C12 muscleconstructs," *JOURNAL OF TISSUE ENGINEERING AND REGENERATIVE MEDICINE*, vol. 2, pp. 279-287, May 2008. doi: 10.1002/term.93.

[42] K. Cole, N. Henao, T. Miller, K. Pawelski. April 2015. “Mechanical and Electrical Stimulation Device for the Creation of a Functional Unit of Human Skeletal Muscle *in Vitro.*”

[43] B. Cossette, A. Goncalves, A. Marry, M. William. April 24, 2017. “High-Throughput Maturation of Engineered Human Skeletal Muscle Tissue.”

[44] R. G. Dennis and P. E. Kosnik, “Excitability and isometric contractile properties of mammalian skeletal muscle constructs engineered *in vitro,*” *In Vitro Cell. Dev. Biol. Anim.*, vol. 36, no. 5, pp. 327–335, May 2000.

[45] “Silk Nitinol.” Fort Wayne Metals, https://www.fwmetals.com/materials/nitinol/silk-nitinol/. Accessed 1 Oct. 2018.

[46] Y.-C. Huang, R. G. Dennis, L. Larkin, and K. Baar, “Rapid formation of functional muscle *in vitro* using fibrin gels,” *J. Appl. Physiol.*, vol. 98, no. 2, pp. 706–713, Feb. 2005.

[47] C. A. Powell, B. L. Smiley, J. Mills, and H. H. Vandenburgh, “Mechanical stimulation improves tissue-engineered human skeletal muscle,” *Am. J. Physiol., Cell Physiol.*, vol. 283, no. 5, pp. C1557-1565, Nov. 2002.

Appendix

Appendix A: Materials and Budget

Materials List & Cost of Used Materials

Component	Cost
3D Printed Prototypes & Final Model	$100
BMP280 Sensors * 8	$45
Arduino Nano	$0 (Available in lab, $4 value)
Arduino Wires & Copper Wiring	$5
Pressure Pumps * 8	$46.50
316 Stainless Steel Needles * 16	$0 (Available in lab, $6.08 value)
Leadless Solder	$10
Silicone Elastomer Kit	$0 (Available in lab, $200 value)
Rubber Stoppers * 8	$2.50
Medical Tubing	$0 (Available in lab, $5 value)
Total Cost	$209.00
Total Cost Value	$424.08

MQP Budget Used: $300.50

- ➔ Bought double sensors
- ➔ Bought double pumps

Appendix B: Arduino Code

```
#include <Wire.h>
#include <SPI.h>
#include <Adafruit_Sensor.h>
#include <Adafruit_BMP280.h>

#define BMP_SCK 13
#define BMP_MISO 12
#define BMP_MOSI 11
#define BMP_CS 10
#define Vacuum1 05

Adafruit_BMP280 sensor; // I2C

//Adafruit_BMP280 bme(BMP_CS); // hardware SPI
//Adafruit_BMP280 bme(BMP_CS, BMP_MOSI, BMP_MISO,  BMP_SCK);

double readSensor(int select){
  digitalWrite(select, HIGH); //turns the selected sensor on
  delay(250);
  sensor.begin(); //initialize and read the sensor pressure value
  sensor.readPressure(); //pressure value is read twice as initial reading is sometimes inconsistent, as
recommended by manufacturers
  delay(250);
  double result = sensor.readPressure(); //read pressure takes the pressure value from the sensor
  digitalWrite(select, LOW); //after the value has been read, turn this sensor off
  delay(1000);
  Serial.print("Pressure: ");
  Serial.print(result);
  Serial.println();
  delay(1000);
  return result;  //returns pressure in KPa (100,000 is approximately 1 atmosphere
}

void stimulationCycle(int select){ //powers up the corresponding electrode
  int pow = 100;
  for (int i = 0; i < 10; i++){
          analogWrite(i+17, pow); //17 pins "above" the digital pins are a set of 8 corresponding analog pins
for writing to
          delay(250);
          pow = pow * readSensor(select)/100000; //generates a new power to electrify with based on the
pressure induced by the electrical stimulation of the muscle. for example, if the pressure increases 1% to
101,000, then 100 * 101,000/100,000 = 101, increasing the electrical stimulation proportionately
          analogWrite(i+17, 0); //shut off electrical stimulation
          analogWrite(16, pow); //this induces pressure on the muscles stretching them
```

```
        delay(250); //a delay is given to allow pressure to build and stretch the muscle
        analogWrite(16, 0); //shut off physical stimulation
  }
}

void setup() {
  Serial.begin(9600);
  Serial.println(F("MQP Multi Test"));
  pinMode(2, OUTPUT); //set these pins to output, so that values can be written
  pinMode(3, OUTPUT);
  pinMode(4, OUTPUT);
  pinMode(5, OUTPUT);
  pinMode(6, OUTPUT);
  pinMode(7, OUTPUT);
  pinMode(8, OUTPUT);
  pinMode(9, OUTPUT);
  //sensor.begin();
}

void loop() {
        for (int i = 2; i < 9; i++){ //pins 2 through 9 were used to separately power each of the 8 sensors.
this will read from each of those sensors
     Serial.println(i);
     stimulationCycle(i);
        delay(250);
        }
    //Serial.println();
        delay(1000);
}
```

Appendix C: Microposts Fabrication

Myomics Inc.
4 Richmond Square, 5th Floor
Providence RI 02906

OPERATING PROCEDURE # DS1.0

TITLE: Preparation of Silicone Plugs for Plating mBAMS
Effective Date: 7/16/08

1.0 Objective:

The objective of this procedure is to describe the steps for making and cleaning silicone plugs to be inserted into a 96 well plate for casting mBAMS.

2.0 Responsibility:

It is the responsibility of all lab personnel to comply with the safety regulations specified and to follow all the steps in this procedure.

Original author: Kirsten Skelly Date: 7/16/08
Revision author: Janelle Spinazzola Date: 5/15/09
Revision author: Stephanie Chery Date: 6/17/10
Revision author: Date:
Revision author: Date:

3.0 Safety:

3.1 Refer to the lab Safety Manual.
3.2 Wear safety glasses and gloves when working with biohazardous material.

4.0 Applicable Documents

5.0 Materials

5.1 Components
5.1.1 Silicone curing agent (Dow Sylgard 184 kit)
5.1.2 Silicone elastomer base (Dow Sylgard 184 kit)
5.1.3 99% Propanol Alcohol
5.1.4 Bioclean detergent
5.1.5 Distilled water
5.1.6 Plug Molds (version SS 3)

5.2 Support Materials

5.2.1 Autoclave tape
5.2.2 Sterilization bags (7 ½ ” x 13” for 2 petri dish)
5.2.3 Gloves
5.2.4 C-clamps
5.2.5 N2 tank (with attachment to the air tight container and blow gun attachment)
5.2.6 Forceps
5.2.7 Glass petri dish
5.2.8 100 ml beaker
5.2.9 Spatulas
5.2.10 Saran wrap
5.2.11 Kimwipes
5.2.12 Razor blade
5.2.13 Pressure gauges

6.0 Equipment

6.1 Sonicator
6.2 Platform Vortex
6.3 Autoclave
6.4 Pressure pump 1/8 horsepower
6.5 Air tight container (to attach to pressure pump) large enough to hold 100 ml beaker and molds,
with 2 arms (1 arm should have a sling to hold the beaker)
6.6 Benchtop Oven
6.7 Balance

7.0 Procedure

7.1 CASTING THE PLUGS (27 plugs per mold):
**** Always wear gloves when working with the plugs and silicone***
7.1.1 Mix alcohol with 1 part curing agent and10 parts elastomer base in 100 ml beaker. (i.e., 1 g 99 % Propanol Alcohol + 4.0 g curing agent + 40.0 g elastomer base). You will need about 18 – 20 g to fill a mold.
7.1.2 Preheat the oven to ~122oC.
7.1.3 Line the bottom of the vacuum box with tinfoil.
7.1.4 Use a mixing spatula to mix the silicone parts together, and then place on the vortex for about 30 secs until it appears well mixed.
7.1.5 Place the beaker with the silicone in the sling of the arm of the vacuum box. You can tighten the sling by turning the screw on the end of the sling.
7.1.6 Insert the teflon piece onto the cap-side of the stainless steel mold and place it in the box adjacent to the beaker.

7.1.7 Close the lid to the box, open the valve on the N2 tank and turn the vacuum on. Make sure the intake valve (big black knob on the left) is turned all the way clockwise and the release valve (small black knob on the right side) is turned to clockwise as well. The Intake valve controls the vacuum and the release valve controls the N2 released into the box.
7.1.8 Once the vacuum is on, turn the intake valve to the left to start vacuuming out the air in the box. Once this starts, vigorously shake the handle holding the beaker left to right with quick motion. This will break the bubbles that form. If not, silicon will bubble up and out of the beaker. You only need to shake until the digital pressure gauge reads below 600 microns, at this point the bubbles will break under their own weight.
7.1.9 Let the silicone sit in the vacuum until the gauge shows below 600 microns. If the pressure gauge slows down or stops before reaching 600 microns, close the intake valve (turn counter clockwise) and open the release valve (turn counter clockwise as well) and bring the pressure up on the smaller gauge attached to the right of the box, to about -5 inHg. Then close the release valve and open the intake valve back up. Repeat this until the digital pressure gauge shows below the 600 microns.
*** Current Digital Pressure Indicator not working***
7.1.10 Once it is below the 600 microns, use the arm with the beaker in the sling and pour the silicone into the mold until it is full.
7.1.11 Using the release and intake valves, increase the pressure again to about -5 inHg and bring the pressure back down again. You want to get the pressure to below 500 microns with little to no bubbles forming in the silicone in the mold.
7.1.12 Once it is below 500 microns with little or no bubbles use the release and intake valves to bring the pressure in the box to room pressure.
7.1.13 Close the lid and lower the pressure in the box. You want to get around 400-500 microns with minimal bubbles (there will always be bubbles now). This part should take 5-10 min.
7.1.14 Once you feel that it is at minimal bubbles, increase the pressure in the box to the room pressure.
7.1.15 Turn off the vacuum and open the lid. Place the teflon top of the mold on the base-side and press firmly to snap into place. Clamp tightly with 3 C-clamps arranged in an alternating pattern.
7.1.16 Place the mold with the clamps in the oven for 30 minutes.

7.2 REMOVING THE PLUGS:

*** Wear gloves when working with the plugs and silicone***

7.2.1 Once the mold has been removed from the oven, remove the clamps and use a mixing spatula and 70% Isopropyl Alcohol to remove the excess silicone that is cured on the mold.
7.2.1.1 Again using the mixing spatula and 70% Isopropyl Alcohol, slowly pry off the cap-side teflon piece.
7.2.1.2 Squirt some 70% Isopropyl Alcohol onto the capside and rub it around.
7.2.2 Now slowly remove the teflon base-side piece using the thick spatula. Most of the plugs should come out stuck to the teflon with caps intact.

7.2.3 Squirt 70% isoporpyl alcohol on the teflon piece and carefully remove the plugs with the forceps.
7.2.4 Line up the plugs on one of the aluminum bars to cool.
7.2.5 Use forceps and/or the dental pick to remove the plugs that did not come out on the teflon. Avoid scratching the stainless steel around the plug caps.
7.2.6 The plugs should have the base, 2 posts and 2 caps intact. Check to make sure the base is without bubbles and the caps are full formed but with no excess silicone on the cap.

7.3 CLEANING THE PLUGS:
7.3.1 Switch on Sonicator
7.3.2 Fill to operating level – tap water is okay when using beakers
7.3.3 Settings: 50degC, Heat on.
7.3.4 Fill one of the steel beakers with ~1-2ml Bioclean soap, concentrated blue and fill 1/2 - 3/4 of the beaker with de-ionized water (DI-water)
7.3.5 Add silicone plugs into beaker
7.3.6 Place beaker in Sonicator, set the degas for 5 min. and turn it on.
7.3.7 After the degas has ran, set the sonics for 30 min. and turn on the sonics.
7.3.8 Remove plugs from beaker with a pair of tweezers.
7.3.9 Add enough dH2O into the beaker to submerge them.
7.3.10 Seal beaker with plastic wrap and place on agitator (Vortex) for a few minutes to exchange liquid on the surface of plugs to wash off soap thoroughly.
7.3.11 Remove plastic wrap and pour out water without losing plugs.
7.3.12 Repeat steps 10-12 until no more soap bubbles are visible.
7.3.13 Add 70% Isopropyl alcohol into the beaker.
7.3.14 Seal beaker with plastic wrap, place on agitator for a few minutes.
7.3.15 Remove plastic wrap and pour out the alcohol.
7.3.16 Seal the beaker with plastic wrap or parafilm, poke a few small holes in the top, and blow N2 into the beaker until plugs appear dry. Be careful not to make the hole too big or they will rip open.
7.3.17 Place plugs onto a clean glass petri dish. Label the dish with # of plugs, Batch #, Mold #, date cleaned and your initials. Place the autoclave tape on sides of dish and place dish in autoclave bag.
7.3.18 Place bags in autoclave. (Instruments setting)
7.3.19 Once they are autoclave, place the bag/plugs under the biological safety cabinet. Date and Initial bag.

Appendix D: Cell Subculturing Procedure

1. Aspirate old media.
2. Rinse with 5 mL DPBS (-) & aspirate.
3. Add 3 mL 0.25% trypsin-EDTA solution.
4. Incubate at 37ºC for 5-10 minutes.
5. Check plate under microscope. If all the cells are loose and rounded, proceed to the next step. If most of the cells are still attached to the plate, reincubate for 5 more minutes and check again. Do not exceed 20 minutes trypsonizing.
6. Add 2 mL of complete medium. Disperse cells by repeated pipetting, avoiding air bubbles.
7. Transfer cell suspension to a sterile 15 mL conical tube. Repeat pipetting to break up any cell clusters.
8. If doing a cell count, take a 7 µL sample of the solution here.
9. Spin the conical tube at 200 G for 5-10 minutes. Make sure the ribbed side of the tube is on the bottom.
10. Aspirate the medium, being careful to not aspirate the cell pellet.
11. Resuspend cells in an appropriate amount of complete medium, depending on the ratio of subculturing or concentration for replating.
12. Plate the desired number of cells or volume of suspension into a fresh plate. Make up total volume to 10 mL.
13. Check cells in microscope.
14. Incubate plate.